Estudios Geológicos
julio-diciembre 2020, 76(2), e134
ISSN-L: 0367-0449
https://doi.org/10.3989/egeol.43508.527

Understanding the Quaternary evolution of an intramountain staircase terraces model using morphometric indices: Lozoya River, Central System, Spain

Estudio de la evolución cuaternaria de un modelado fluvial escalonado intramontañoso mediante índices morfométricos: río Lozoya, Sistema Central Español

Theodoros Karampaglidis[1,*], Alfonso Benito-Calvo[2], Alfredo Pérez-González[3]

[1]MONREPOS, Archaeological Research Centre and Museum for Human Behavioural Evolution, Schloss Monrepos, 56567 Neuwied, Germany. ORCID ID: https://orcid.org/0000-0001-5626-4548
[2]Centro Nacional de Investigación sobre la Evolución Humana (CENIEH), Paseo Sierra de Atapuerca, 3. 09002 Burgos, Spain. ORCID ID: https://orcid.org/0000-0002-6363-1753
[3]I.D.E.A. The Institute of Evolution in Africa, Calle Covarrubias 36, 28010 Madrid, Spain. ORCID ID: https://orcid.org/0000-0003-1122-9313
*Corresponding author: teokaram30@gmail.com

ABSTRACT

Morphometric indices have been described as useful tools to understand the geodynamic evolution in different spatial regions and contexts, although usually only current landform shapes are considered when applying them. In this work, we combined detailed geomorphological mapping and the most representative morphometric indices and variables (valley width to valley height ratio Vf, transverse topographic asymmetry factor T-index, stream length–gradient SL, concavity index CI, elevation & slope), to quantify the evolution of the Lozoya valley landscape. These indices were not only applied to present landforms. In the case of Vf, this was measured also for different periods using the paleotopographies defined by the fluvial rock terraces. These techniques were applied to the Lozoya rock terrace staircase using a Geographic Information System (GIS) and statistical tools. This area developed in an intramountain tectonic depression delimited by basement pop-up alignments (Central System, Spain). The geomorphometric analysis revealed a complex Quaternary evolution controlled by Alpine structures, subsoil lithology, regional geomorphology, uplift and climatic factors. More incised valley shapes are located downstream, associated with lithostructural changes and fluvial captures, whereas upstream the valley displays a wide geometry coinciding with the pop-down depression. The more marked incisions are related to knickpoints identified in the Lozoya longitudinal profile, which persist through time from at least the Late Miocene and apparently did not undergo Quaternary reactivation. Finally, our analysis reveals lithological and morphostuctural controls to Lozoya bedrock terraces formation and preservation.

Keywords: Morphometric analysis; fluvial incision; rock terraces; Lozoya River; Spanish Central System

Recibido el 7 de febrero de 2019; Aceptado el 7 de septiembre de 2020; Publicado online el 18 de noviembre de 2020

Citation / Cómo citar este artículo: Karampaglidis, T. et al. (2020). Understanding the Quaternary evolution of an intramountain staircase terraces model using morphometric indices: Lozoya River, Central System, Spain. Estudios Geológicos 76(2): e134. https://doi.org/10.3989/egeol.43508.527.

RESUMEN

Los índices morfométricos son descritos como herramientas útiles para comprender la evolución geodinámica de diferentes regiones geológicas, aunque suelen aplicarse considerando sólo la geometría actual de las formas del relieve. En este trabajo, hemos combinado una cartografía geomorfológica detallada & algunos de los índices y variables morfométricas más relevantes (Vf, Índice-T, SL, concavidad, elevación y pendiente), para cuantificar la evolución del río Lozoya. Estos índices fueron calculados usando no sólo las formas actuales del relieve, sino también para diferentes periodos. Este es el caso del índice Vf, cuyos valores fueron calculados a lo largo del tiempo, utilizando la paleotopografía definida por las terrazas fluviales rocosas del río Lozoya. Estas técnicas fueron aplicadas a la sequencia de terrazas rocosas del río Lozoya por medio de SIG y herrameintas estadísticas. El área de trabajo se ubica en una depresión tectónica intramontañosa delimitada por alineaciones *pop-up* (Sistema Central Español). El análisis geomorfométrico ha revelado una evolución Cuaternaria compleja controlada y condicionada por factores como las principales, estructuras Alpinas, la litología de subsuelo, la geomorfología regional, el levantamiento regional y el clima. En la cuenca de drenaje del Río Lozoya, los valles más incididos y estrechos se localizan aguas abajo, asociados con cambios litoestructurales y capturas fluviales, mientras que los valles más amplios se localizan hacia la zona de cabecera, relacionados con depresiones tectónicas *pop-down*. Por otro lado, el análisis del perfil longitudinal del Río Lozoya ha mostrado que los *knickpoints* mayores han persistido durante el tiempo, por lo menos desde el Mioceno Superior y sin aparentes signos de reactivación durante el Cuaternario. Finalmente, nuestro análisis revela que la formación y preservación de las terrazas erosivas están controladas por factores litológicos y morfoestucturales.

Palabras Clave: Análisis morfométrico; incisión fluvial; terrazas rocosas; Río Lozoya; Sistema Central español

Introduction

Geologists have always speculated about the close relationship between terrain morphology and understanding the principal mechanisms of how the landscape evolved. As technology advances, more and more geomorphologists are using GIS and statistical tools to attempt to quantify and explain how tectonic settings, lithological variety and climatic fluctuations influence the formation and evolution of the terrain. By analyzing drainage basin morphology, mapping fluvial terrace sequences, identifying changes in valley width and reconstructing longitudinal profiles, it is possible to recognize how bedrock uplift from crustal movements or cyclic fluctuations from climatic changes could influence fluvial landscape (Bridgland, 2000, Bull, 2007).

Along these lines, many studies of the Quaternary landscape evolution of the internal basins of the Iberian Peninsula have been carried out (Silva *et al.,* 1988; Pérez-González, 1994; García-Castellanos *et al.,* 2003; Benito-Calvo & Pérez-González, 2008; Cunha *et al.,* 2008; Benito-Calvo & Pérez-González, 2010; Antón *et al.,* 2012; García-Castellanos & Larrasoaña, 2015; Silva *et al.,* 2017; Soria-Jáuregui *et al.,* 2018; Cunha *et al.,* 2019; Struth *et al.,* 2019; Gouveia *et al.,* 2020; Rodríguez-Rodríguez *et al.*, 2020). Likewise, this paper analyzes the Quaternary landscape geometry and evolution of the Lozoya intramountain basin located in the eastern part of the Spanish Central System (SCS), which presents a complex morphostructural evolution (Figure 1; Hernández-Pacheco 1932; Schwenzner, 1937; Birot & Solè Sabaris, 1954; Gladfelter, 1971; Pedraza, 1978; Garzón Heydt, 1980; Gracia *et al.,* 1988; Pérez-González, 1994; Gutiérrez-Elorza & Gracia, 1997; Silva & Ortiz, 2002; Alonso-Zarza *et al.,* 1993; Vicente *et al.,* 2007; Benito Calvo & Pérez-González, 2010; Vicente *et al.,* 2011; Karampaglidis, 2015; Silva *et al.,* 2017; Karampaglidis *et al*., 2020). The Lozoya River is a tributary of the Tajo, which is the longest river (1007 km) in the Iberian Peninsula and one of the largest systems of western Europe. In the Tajo basin, a spread Quaternary staircase system has been identified, with up to twelve levels in the western part of the Madrid Cenozoic Basin (MCB) (Pérez-González, 1994), up to twenty-three terrace levels in the eastern part of the MCB (Pérez-González, 1994) and up to six levels in the Lower Tajo Basin (Cunha *et al.,* 2008). These terrace records are attributed to the main fluvial system which dissects the Tajo basin. These long-term staircase terrace systems are appropriate for understanding the principal mechanisms of the landscape evolution (Antoine *et al.,* 2000; Bridgland, 2000; Van den Berg & Van Hoof, 2001; Westaway *et al.,* 2002, 2006; Bridgland & Westaway, 2008) driven by combinations of tectonics, climate and eustacy (Bridgland & Westaway, 2008).

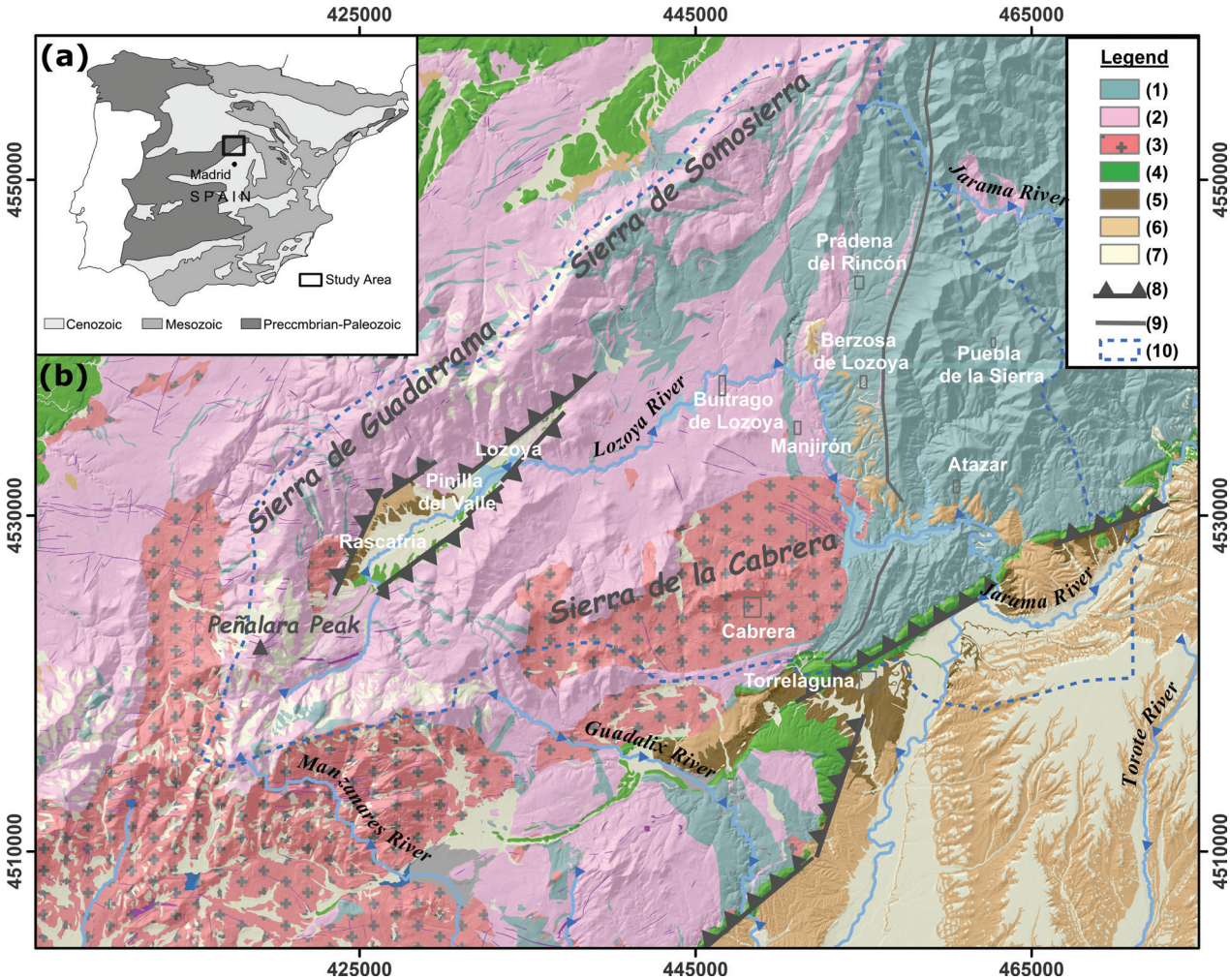

Figure 1.—(a) Location of the study area situated in the Central Iberian Peninsula (Spain). (b) Simplified geological map of the Lozoya River valley, modified from Arenas *et al.* (1991); Azor *et al.* (1991); Bellido *et al.* (1991a, 1991b); Aznar *et al.* (1995); Bellido *et al.* (2004); Pérez-González *et al.* (2010); Karampaglidis *et al.* (2014a). Legend: (1) Paleozoic (paragneiss, schist, psammite, black slate and quartzite), (2) Ordovician (orthogneiss and leucogneiss), (3) Variscan (granite and adamellite), (4) Permian (hypabyssal rocks), (5) Mesozoic (sandstone, sand, dolomite and lutite), (6) Paleogene (conglomerates and sands), (7) Neogene (boulders, cobbles, sands and clays), (8) Quaternary (gravels, sands, silts and clays), (9) Thrust faults, (10) Faults, (11) Study area.

To contribute to these questions, we carried out a detailed geomorphological study applying geomorphometric indices. Using these indices and geomorphological analysis to study uplift processes, incision, lithostructural controls, climatic events or fluvial captures is a technique that has been applied successfully for years in landscape evolution studies (Horton, 1945; Strahler, 1964; Hack, 1973; Bull & McFadden, 1977; Garzón Heydt, 1980; Silva *et al.,* 1988; Ritter *et al.,* 1995; Garrote *et al.*, 2002; McKnight & Hess, 2005; Garrote *et al.*, 2008; Türkan & Bekir, 2011; Antón *et al.,* 2014; Soria-Jáuregui *et al.,* 2018). Terrain evolution is thought to converge towards a dynamic equilibrium between uplift and incision (Burbank & Anderson, 2001). The effects of this balance remain recorded in the terrain topography, which is used to infer geodynamic processes through geomorphometric index analysis (Patton, 1988; Vijith & Satheesh, 2006; Jena & Tiwari, 2006).

The indices are based on the morphometric parameters of landforms calculated from the current relief topography, usually expressed on maps or in DEMs. Using the current topography provides mean values corresponding to the whole landform formation, or

values reflecting the recent situation. Nevertheless, geomorphometric analysis can also be applied to residual landforms based on the reconstruction of geomorphic levels, providing useful information about how landforms have evolved over time. In this study, we have applied this method to assess the morphostructural influence on the Lozoya watershed. This area is suitable for this kind of analysis because the following are well defined: (i) the pre-Quaternary planation surfaces which mark the beginning of the Quaternary exorheic fluvial system; (ii) a robust, complex staircase fluvial system established by the Lozoya, Jarama, Henares, Tajuña and Tajo rivers is preserved; (iii) fairly well-studied Late Cenozoic sedimentary sequences; and (iv) the tectonic activity is well-documented. Geomorphometric analysis was performed using the Vf index and stream longitudinal profile analysis, through the SL and CI indices. Slope and curvature variability have also been used along stream profiles.

Study area

The drainage basin of the Lozoya River constitutes an intramountain tectonic depression (SCS; Figure 1a), developed between two mountainous alignments uplifted as a pop-up mountain range during the Alpine orogeny: the ENE-WNW Guadarrama–Somosierra mountains to the North, and the ENE-WNW Sierra de la Cabrera to the South (Figure 1b; Vicente *et al.,* 2007). The Lozoya watershed covers 925 km^2, with the highest elevation at the peak of Peñalara (2428 m, Sierra de Guadarrama), and the lowest altitude in the area where the Lozoya meets the Jarama River (Figure 2 (a); 700 m). The Lozoya is a tributary of the Jarama, which flows in turn into the main collector of the basin, the Tajo.

Geological setting

The main lithologies which outcrop in the Lozoya watershed are the Paleozoic rocks of the Iberian Massif (Figure 1b). The oldest rocks consist of metasediments, paragneiss, quartzites and marbles of Precambrian age, situated to the NE (Arenas *et al.,* 1991; Bellido *et al.,* 1991a, 1991b). In the eastern segment, schists, quartzites and shales of Ordovician and Silurian age outcrop (Capote & Fernández, 1975), whereas the south is characterized by pre-Permian granites and adamellites. All these lithologies were affected by penetrative schistosity and folding during the Variscan orogeny (Arenas *et al.,* 1991; Bellido *et al.,* 1991a, 1991b). During the Permian, dikes of porphyry, lamprophyre, quartz, microdiorite and aplite were emplaced in the SE segment. Mesozoic deposits are located in contact with the Madrid Cenozoic Basin and in the Upper Lozoya Valley (pop-down depression) (NE segment). The base of these Cretaceous deposits is composed of fluvial sediments, the so-called Facies Utrillas (clays, gravels, lutites, carbonates, sandstones and dolomites), overlain by sands, lutites, carbonates, sandstones and dolomites deposited during the Turonian-Santonian marine transgression (Aznar *et al.,* 1995). Above the Cretaceous sequence, there are lake deposits and gypsum. At the beginning of the Alpine movements (Paleocene), conglomerates with Mesozoic calcareous boulders were deposited. This episode corresponds to a period of thrusting before the arkosic filling of the Cenozoic basins (Capote *et al.,* 1987). In the Pinilla del Valle area and to the west, Miocene detritic alluvial sediments are present. The Miocene is characterized by thrusting generating NE-SW structures and folding of the Mesozoic and Cenozoic deposits in the Iberian Mountain range (Vicente *et al.,* 2007). Finally, several impulses of vertical uplifting as a result of regional extensional stresses have been defined in different parts of the SCS during the Pliocene and up to the present day (De Bruijne & Andrienssen, 2002; Vicente *et al.,* 2007). However, in this sector, there is no evidence for neotectonic activity or historic seismicity (Baena-Perez *et al.,* 1998; http://www.ign.es/ign/layoutIn/sismoTerremotosEspana.do). Quaternary landforms in the Lozoya watershed are mainly erosive: deposits located and associated with fluvial and glacial processes, colluviums, peat formations, solifluction formations and karstic environments have been described in several studies (Pedraza, 1994; Torres *et al.,* 1995; Torres *et al.,* 2005; Arsuaga *et al.,* 2006; Pedraza & Carrasco 2005; Pérez-González *et al.,* 2010; Palacios *et al.,* 2011).

Quaternary fluvial geomorphological features and stratigraphic data

The main landforms identified in the Lozoya watershed can be grouped as erosive surfaces**,** polygenetic residual features (inselbergs, glacis), fluvial morphologies (e.g. strath terraces, rock terraces or alluvial fans), glacial landforms (e.g. cirques, moraines), karstic features (e.g. caves, dolines, karren, karstic infillings), and gravity forms (Karampaglidis *et al.,* 2014a).

Our work is focused on the Quaternary fluvial landforms (Figures 2, 3 & 4), which form an erosive terrace staircase arrangement (Karampaglidis *et al.,* 2014a). According to the characteristics and distribution of these glacis and terraces, together with the morphostructural

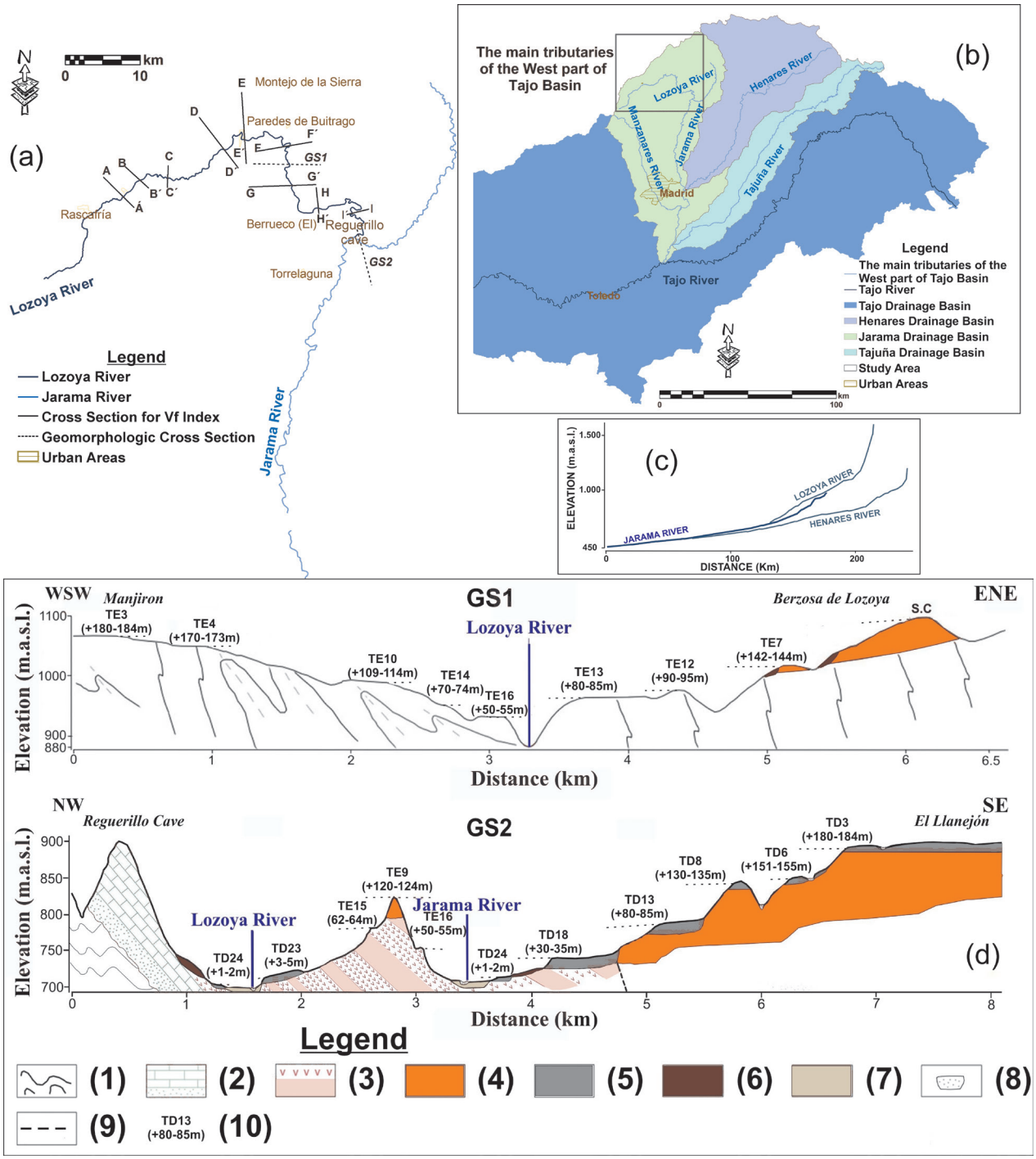

Figure 2.—(a, b) The Lozoya River and the main tributaries of the western part of the Tajo Basin. (c) Jarama, Henares and Lozoya River longitudinal profiles. (d) Transverse geomorphological section for the Lozoya River (GS1) and Jarama River (GS2). Legend: 1. Gneiss and metasediments (Paleozoic), 2. Dolomites, sandstones, sands and clays (Cretaceous), 3. Red siltstone (Paleocene), 4. Boulders and cobbles of gneiss, psammite and quartzite (Neogene), 5. Fluvial terraces (Quaternary), 6. Colluvium (Holocene), 7. Floodplain (Holocene), 8. Current river channel, 9. Fault, and 10. Terrace levels.

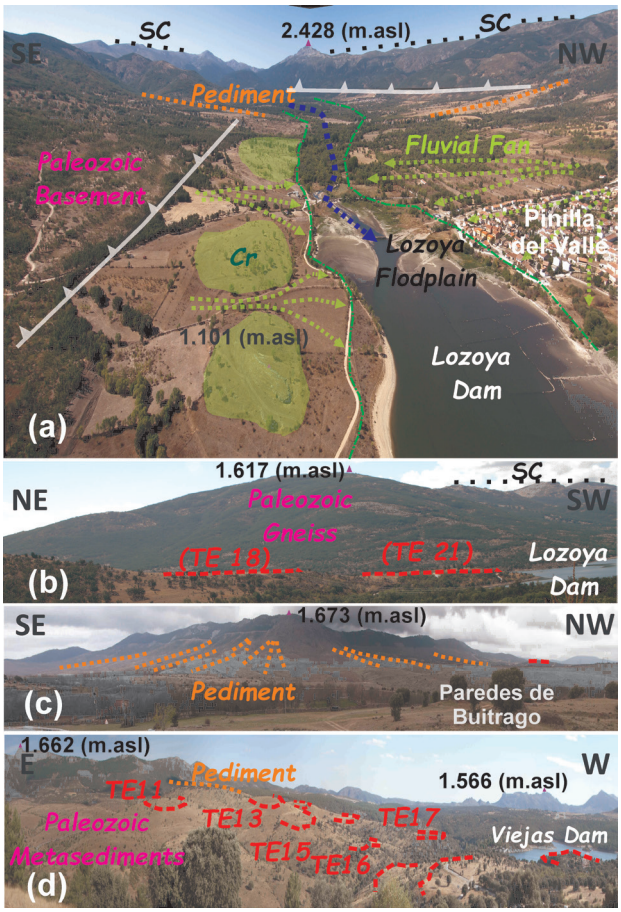

Figure 3.—(a) Panoramic view of the northern part of the tectonic depression in the Pinilla del Valle sector delineating the main geomorphological features. (b) Panoramic view of the western part of the tectonic depression in the Pinilla del Valle sector delineating the main geomorphological features. (c) Panoramic view delineating the erosive pediments in the Paredes de Buitrago (Buitrago de Lozoya sector) area and the alluvial pediment (G4) at the village of Berzosa de Lozoya: the level names and numbers are after Benito-Calvo and Pérez-González, 2010 and Karampaglidis, 2015. (d) Panoramic view of the Viejas dam area (Berzosa de Lozoya; Buitrago de Lozoya sector) delineating the Lozoya River rock terrace staircase sequence.

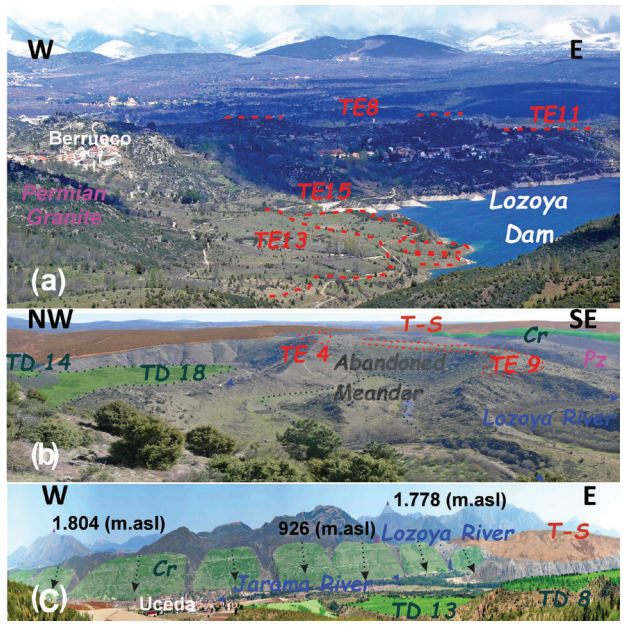

Figure 4.—(a) Panoramic view of the Berrueco village area (Atazar sector) delineating the Lozoya River rock terrace staircase sequence. (b) Panoramic view of the principal fluvial geomorphological features of the Lozoya River on black slates (Ponton de la Oliva sector). (c) Panoramic view of the principal geomorphological features at the confluence of the Lozoya River with the Jarama River. Abbreviation: TE – Rock terrace; TD – Strath terrace; T-S – Turolian sediments; Cr – Cretaceous dolomites and limestones; Pz: Paleozoic rocks.

and bedrock characteristics of the valley, we have divided the Lozoya watershed into four sectors: the Pinilla del Valle sector, the Buitrago de Lozoya sector, the Atazar sector and the Cerro de la Oliva sector (Figure 3, 4 & 5; Karampaglidis *et al.,* 2011).

The first sector of the watershed (Pinilla del Valle) is a NE-SW pop-down tectonic depression (Warburton & Alvarez, 1989; Vicente *et al.,* 2007), which determines the slope distribution and the main direction of the Lozoya River in this area (Figure 5). The geology here is characterized by soft Mesozoic and Cenozoic sedimentary rocks. In this sector, the fluvial style of the Lozoya River changes from a shallow gravel braided facies model to a meandering gravel-bed facies model. The river load is characterized by clastic rocks and polygenic composition (metamorphic and igneous rocks: Figure 1). In this area, the earliest terraces and glacis are erosive, degraded and with reduced dimensions, developing on the Paleozoic metamorphic rocks between T2 (+190-195 m) and T15 (+62-64 m). Below them, rock terraces and glacis between T16 (+50-55 m) and T20 (+17-20 m) are preserved on Mesozoic and Cenozoic rocks. This sector is one of the few areas where fluvial deposits are located, composed of cobbles, coarse-medium gravel, sands and muds corresponding to strath terraces, alluvial fans and fluvial deposits preserved in a karstic system (Pinilla del Valle caves) (Figure 3). In this karstic system, we have observed three episodes of fluvial aggradation situated at +23-25 m (T19), +11-14 m (T21), and +7 (T22) (Karampaglidis *et al.,* 2014a). The second episode (T21, +11-14 m) was dated by thermoluminescence (TL) on quartz grains at 140.4 ± 11.3 ka B.P., while the deposits at +7 m (T22) have an age of 59.4 ± 4.7 ka B.P. (Thermoluminescence Laboratory, Universidad Autónoma de Madrid; Pérez-González *et al.,* 2010). Furthermore, two other levels of

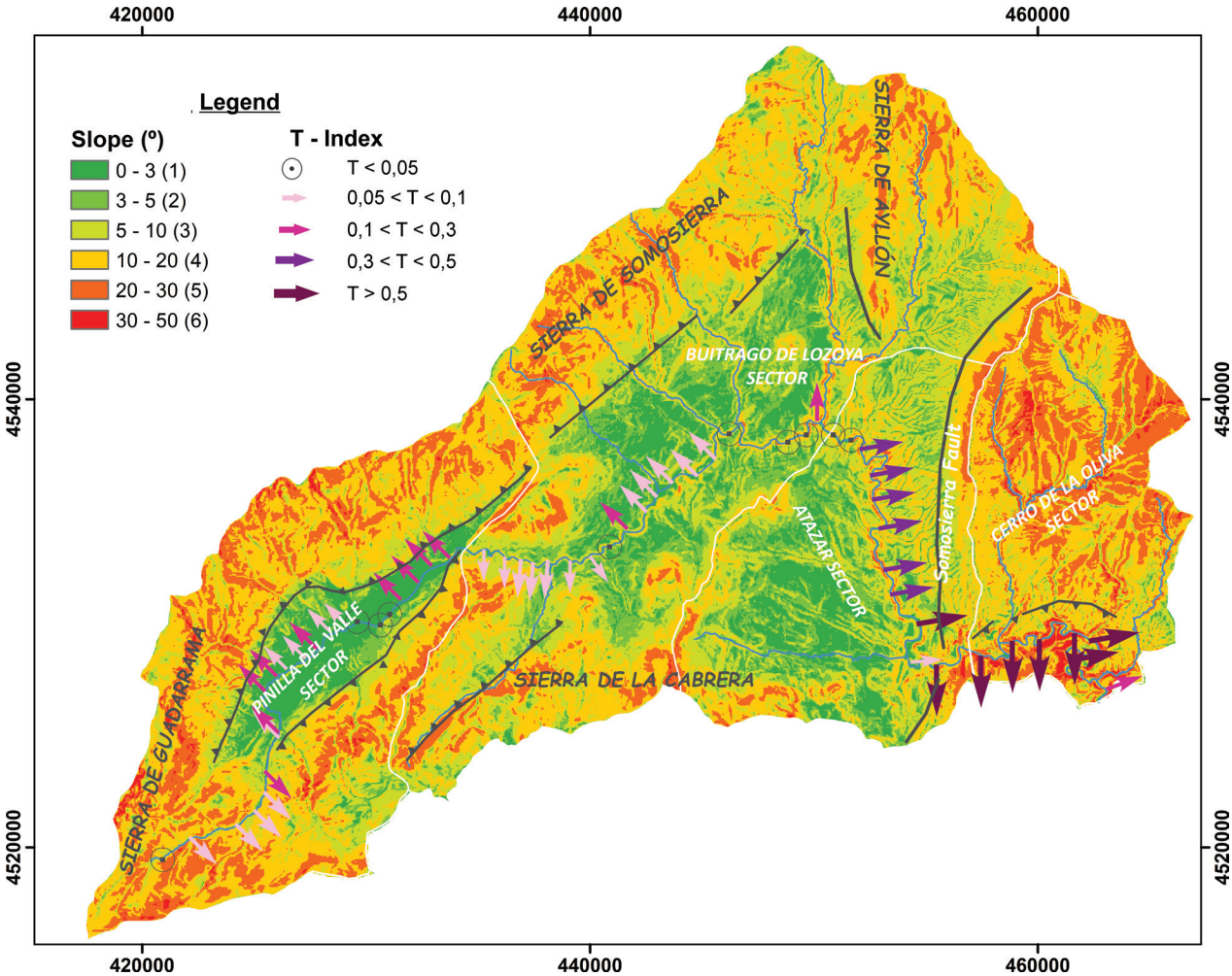

Figure 5.—Slope map, T-index and its distribution in the four sectors differentiated according to their geomorphological, lithological and structural characteristics in the Lozoya watershed. The gray line represents faults (Somosierra Fault) and the gray line with triangles shows local thrusts.

strath terraces (T23, +3-5 m & T24, +1-2 m) were identified in this sector. The deposits of T23 were dated at 17,950 ± 1.1 ka B.P. using accelerator mass spectrometry (AMS) in organic sediments (Karampaglidis *et al.,* 2014a). The stream load energy may increase as a result of climate change and/or tectonic activity (Merrits *et al.*, 1994; Pazzaglia *et al.*, 1998). In this sector, local fluvial deposit formation of the last two terrace levels (T22, +7 m & T23 +3-5 m) and valley widening coincide with some of the well-documented periods of local glaciation (19 ka) or cold periods (~60 ka) (Carrasco *et al.*, 2016).

In the second sector (Buitrago de Lozoya), the course of the Lozoya River can be classified as an incised meander bedrock river (sinuosity of 2.71; Karampaglidis et al., 2011), entrenched from T18 (+30-35 m), showing a NE-SW general direction following the NE-SW trends of the SCS pop-up structure (Vicente *et al*., 2007). In this sector, most of the preserved terraces are erosive and the oldest terraces and glacis are poorly preserved. The surface of the terraces and glacis is characterized by rock-weathering material, such as angular blocks and clasts, with a fine soil covering of 3-4 cm thickness. Occasionally, low terraces (T23, +3-4 m, & T24, +1-2 m) contain 40-50 cm of rounded oligomictic boulders and cobbles, sands and silts (Karampaglidis *et al.,* 2014a). Towards the north, river captures were identified associated with the evolution of the Madarquillo River (Figure 1). Part of this river is the Hontanar stream which presents an unexpected mature-stage meander higher than the local base level of the Valle stream, a short local linear stream situated on the structural contact between gneiss and metasediments (Paleozoic) (Figure 6). The second capture is related

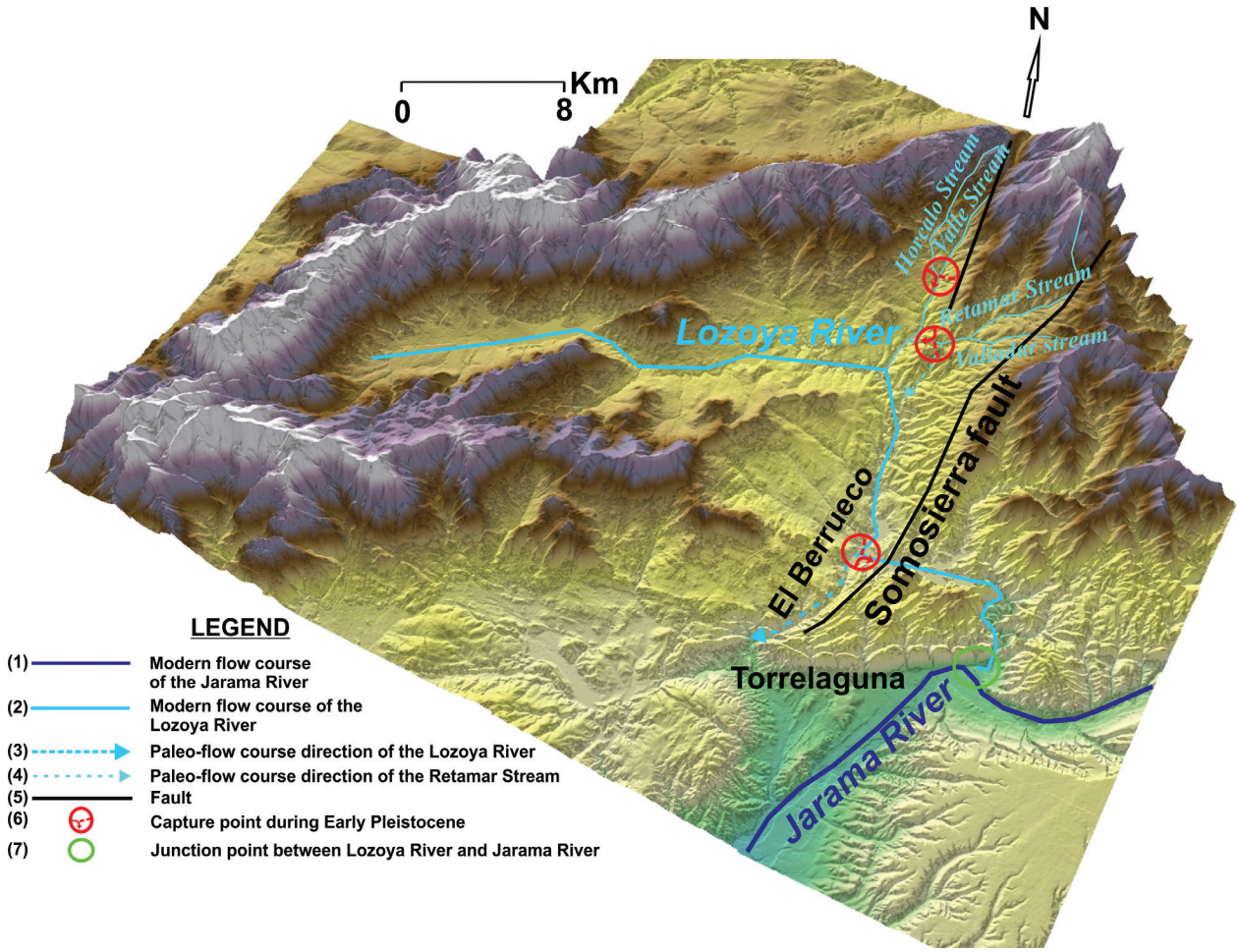

Figure 6.—Early Pleistocene fluvial captures in the Lozoya watershed. (1) Modern course of the Jarama River, (2) Modern course of the Lozoya River, (3) Paleoflow course of the Lozoya River, (4) Paleoflow course of the Retamar stream, (5) Fault, (6) Capture point during Early Pleistocene and (7) Confluence of Lozoya and Jarama rivers.

to the parallel valley of the Retamar stream (Figure 6). This is a hanging fluvial valley captured from the Valle stream. These captures are related to greater incision, produced when the Valle stream incised the structural contact and/or by fault reactivation, and probably occurred after T13, +80-85 m (Early Pleistocene), since this is the last common rock terrace (Karampaglidis *et al.,* 2011; Karampaglidis, 2015).

In the Atazar sector, the morphology of the Lozoya River is controlled by E-W and N-S fractures (Figure 1 & 2a), and this explains its N-S direction of flow in the southern part of this sector. The valley describes incised meanders entrenched from T13 (+80-85 m), displaying a sinuosity of 2.68 (Figure 5; Karampaglidis *et al.,* 2011). In this sector, rock terraces and glacis sequences are located on the Paleozoic rocks and on Neogene deposits (Figure 1 & 3). The youngest Neogene deposits appear in this sector, forming a surface perched about +220 m above the present river channel (Figure 1, 3 & 4). Below this level, fluvial rock terraces are preserved on the Pliocene deposits (from T1, +200-205 m to T7, +142-144 m), and on Paleozoic and Permian rocks, where the granites are often affected by weathering processes (Karampaglidis *et al.,* 2014a). In the lower part of this sector, a fluvial capture was recognized (Figure 6), changing the direction of the Lozoya River. During the formation of the first terraces between T1 (+200-205 m) and T4 (+170 m), the Lozoya River drained towards the south through the El Berrueco Pass (Figure 2 & 6). In the subsequent phase, the river and its tributaries were captured, changing the flow direction to the east (Figure 6), where the lower sector develops (Karampaglidis *et al.,* 2011). This capture was recognized during the morphostatistical reconstruction of the Lozoya River base levels and from geomorphological

evidence. Large planation surfaces are suspended above the current base level and the present local tributaries cannot explain their formation (Karampaglidis *et al.,* 2011). This capture probably occurred by local fault reactivation from southern border activity, Early Pleistocene climatic fluctuations and/or headward erosion, which is related with higher incision rates and was produced during the Lozoya River's incision into the regional structural contact between gneisses, granites and black slates (Figure 1).

The lowest sector, or Cerro de la Oliva sector, is characterized by higher incision (Figure 5), forming canyons developed from T5 (+160-165 m), with the highest sinuosity (3.36; Karampaglidis *et al.,* 2011), where fluvial meandering and meander cutoffs have been mapped. In this area, the rock terraces are located on Paleozoic black shales and Neogene deposits. In addition, strath terraces were identified at T16 (+50-55 m), T18 (+30-35 m), T19 (+25 m), T22 (+6-8 m) and T23 (+3-5 m) levels (Figure 4; Karampaglidis *et al.,* 2014a). Fluvial deposits are also preserved in karstic systems (Reguerillo Cave), hanging +140 m above the actual base level of the modern Lozoya River (Figure 2). This deposit contains polymict (igneous and metamorphic rocks) sands, silts and clays, deposited by the Lozoya River (Torres *et al.,* 2005). Those authors have undertaken various measurements of residual magnetism in these deposits, characterized by a sequence of five samples of normal polarity. This magnetostratigraphic sequence and the position of this fluvial level in the regional sequence (Figure 7) suggest an Olduvai subchron age (1.77 ka to 1.95 ka) for these fluvial deposits. This karstic system also contains fluvial deposits in a level at +45 m, below a speleothem dated by ESR at 981 ± 76 ka B.P. (Torres *et al.,* 2005). This age could suggest that this terrace is older, although the date is inconsistent with the

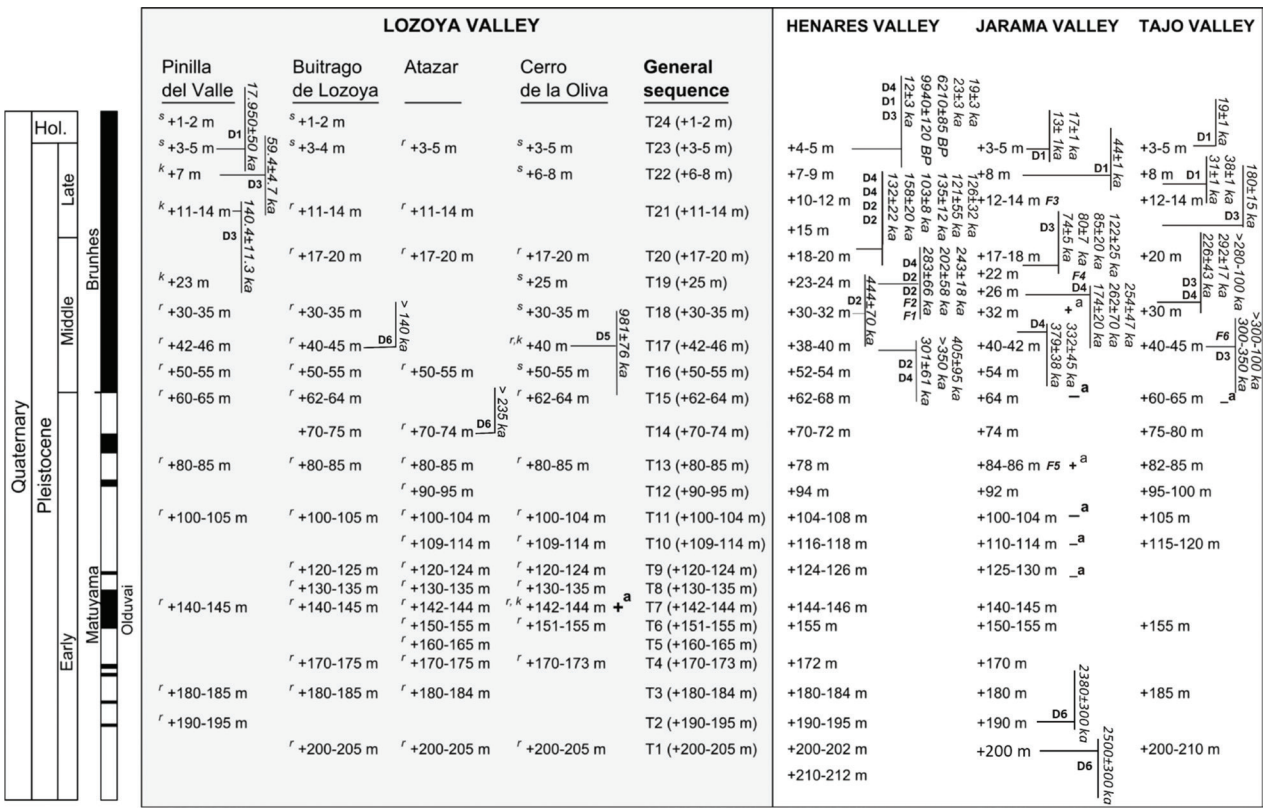

Figure 7.—Lozoya River terrace sequence and its correlation with the sequences of the Tajo River and tributaries, considering relative terrace altitudes, paleomagnetic data, paleontological data and numerical ages. Legend: Numerical dating: ^{14}C (D1), U/Th (D2), TL (D3), Amino acid racemization dating (D4), ESR (D5) and Cosmogenic nuclides (D6). Paleontological data: *Elephas* sp. (F1), *Equus* sp. (F2), *Cervus elaphus* (F3), *Elephas antiquus* (F4), *Mammuthus meridionalis* (F5), *Mammuthus trogontherü, Equus caballus, Hipopotamus amphibius, Dolichodoriceros savini, Eliomys quercinus*, *Allocricetus bursae*, *Microtus brecciensis* and *Apodemus* cf. *sylvaticus* (Sesé & Ruiz, 1992) (F6). (a) Paleomagnetism data: normal polarity (+); reversed polarity (–). Terraces: (s) Strath terrace, (r) Rock terrace and (k) Karstic fluvial deposits. Modified from Ordoñez *et al.* (1990), Pérez-González (1994), Pinilla *et al.,* (1995), Santonja and Pérez-González (1997), Benito *et al.,* (1998), Santonja and Pérez-González (2001), Ortiz *et al.* (2009), Pérez-González *et al.* (2012), Karampaglidis *et al.,* (2014c), Silva *et al.*, 2017, and Karampaglidis *et al.*, 2020.

rest of the chronological trend observed for the sequence in the MCB (Santonja & Pérez-González, 2001; Ordoñez *et al.,* 1990; Ortiz *et al.,* 2009, Silva *et al.*, 2017), which placed terraces at +42-46 m in the Middle Pleistocene. In addition, the paleontological remains found there do not support this age (Figure 7; Sesé & Ruiz, 1992; Morales *et al.,* 1993).

The chronological datasets available for the terraces of the Lozoya valley, and the correlation of this sequence with the main watercourses of the basin (Henares, Jarama and Tajo rivers, Figure 7) (Pérez-González, 1994; Santisteban & Schulte, 2007; Benito-Calvo & Pérez-Gonzalez, 2010; Silva *et al.,* 2017; Karampaglidis *et al.,* 2020) allow us to place the terraces perched up to +3-5 m in the Holocene, and between this and +13-15 m in the Upper Pleistocene. In the Middle Pleistocene, the terraces would be those located from T21 (+11-14 m) up to T16 (+50-55 m), since the level T15 (+60-65 m) has been placed in the Matuyama chron (Pérez-González *et al.,* 2012; Silva *et al.*, 2017), showing reversal of magnetostratigraphic polarities in the Jarama valley. These chronologies are consistent with ages obtained in other valleys in Central Spain (Arlanzón River, Duero Basin), where terraces at +70-78 m have been dated at about 1.14 Ma, levels at +60-67 m at 0.85 Ma, and terraces at +50-54 m at 0.67 Ma (Moreno *et al.,* 2012). The sequence of negative polarities in the Jarama valley could place the terraces T9 (+120-124 m), T10 (+109-114 m) and T11 (+100-104 m) between 1.24-1.77 Ma (Figure 7), whereas the normal polarities obtained in the Lozoya fluvial terrace located in the Reguerillo Cave (Torres *et al.,* 2005), could place terrace T7 (+142-144 m) in the Olduvai subchron, providing older Early Pleistocene ages for the upper terraces. Finally, T1 (+200-205 m), T2 (+190-195 m) and T3 (+180-184 m) could be assigned to the beginning of the Early Pleistocene where terraces close to the junction with the Jarama River are dated between 2.58 Ma and 2.3 Ma (Karampaglidis *et al.,* 2020).

Materials and methods

This study was carried out by combining detailed geomorphological analysis and morphometric indices, which were applied using a GIS (ArcGIS 10) and a 5 m resolution

Table 1.—Descriptive morphometric indexes applied to the Lozoya basin.

Morphometric parameter	Definition	Formula	Description	Parameters	Reference
Vf	Valley floor-Valley height ratio	Vf=2*Vfw/ (Eld-Esc)+ (Erd-Esc)	This index describes the form or shape of the valley cross-section and the degree of maturity of the valley	Vfw:width of valley floor Eld:elevation of the left part of the valley Erd:elevation of the right part valley Esc:elevation of the valley floor	Bull, 1978 Bull & Mc Fadden, 1977 Wells et al., 1988
SL	Stream Length-Gradient index	SL=(H1-H2)/ (lnL2-lnL1)	SL index has been widely used as a profile xy to identify areas of anomalous uplift within landscape.	H1 and H2 are the elevations of each end of a given reach L1 and L2 are the distances from each end of the reach to the source	Hack, 1973
CI	Concavity Index	CI= Σ(Hi*-Hi)/N	The Concavity Index was used to analyze the general shape of the longitudinal profiles	where Hi is the elevation at distance i, Hi* is the elevation along a straight line from the uppermost to lowermost point along the stream line at horizontal distance i, and N is the total number of measurement points	Phillips & Lutz, 2008
T	Transverse topographic asymmetry factor	T=Da/Dd	This index permits to identify rivers lateral migrations related with lithology changes, tectonic activity and climatic fluctuations	Da: Distance from midline of drainage basin of active channel Dd: distance from basin midline to basin divide	Cox, 1994

DEM, created from 1:5000 topographic maps (Comunidad Autónoma de Madrid). Geomorphological mapping was also performed (Karampaglidis *et al.,* 2014a). This map and the DEM have been useful in reconstructing the fluvial base levels, which were used to analyze the variation in geomorphometric indices (Table 1), not only spatially, but also temporally, during the Quaternary evolution of the Lozoya valley. The following morphometric methods were used to analyze the shape evolution of the valleys and the longitudinal stream profile curvature.

Transverse topographic asymmetry factor (T-index)

Asymmetry of drainage basins can be used in homogeneous areas to identify rivers' lateral migrations driven by lithology-structural changes, tectonic activity and climatic changes (Cox, 1994; Garrote *et al.*, 2008; Mink *et al.*, 2014).

$$T = Da/Dd$$

where Da is the distance from the drainage basin midline to the active channel and Dd is the distance from the basin midline to the basin divide.

T-index values vary from 0 to 1, where values close to 0 indicate perfect symmetry whereas those nearer 1 mean maximum asymmetry. The T-index can detect basin asymmetry by quantity (0 to 1) and the direction of lateral stream migrations (Cox., 1994; Garrote *et al.*, 2008; Vijith *et al.*, 2017). In this study, the T-index was applied only to the total length of the Lozoya River (Figure 5).

In order to assess lithological control over all these morphometric parameters, the discriminant analysis statistical technique was also applied.

Valley width to valley height ratio index (Vf)

This is a shape index for the valley cross-section and describes the degree of maturity of a valley (Bull & McFadden, 1977).

$$Vf = 2*Vfw/[(Eld-Esc) + (Erd-Esc)]$$

where Vfw: width of valley floor, Eld: elevation of the left part of the valley, Erd: elevation of the right part of the valley, and Esc: elevation of the valley floor. For Vfw, we have applied the maximum distance between the preserved fluvial terraces on each side in transverse profiles. For Esc, we have utilized the height of the fluvial base level, and for Eld and Erd, the difference in elevation between the terraces considered in each period (Figure 8 & 9).

Typically, this index has been used to distinguish V-shaped valleys (Vf values close to 0), usually associated with linear and rapid fluvial incision related to rapid uplift, from U-shaped and flat-floored valleys (high Vf values), related to less incision, and favoring infilling and sedimentation processes (Seong *et al.,* 2008; Pedrera *et al.,* 2009). In our study, Vf values were calculated in nine sections along the Lozoya River (Figure 8). Our goal was to apply this index along the entire longitudinal profile in all the areas. Based on reconstruction of the Lozoya fluvial base levels defined by the terrace sequence, we were able to calculate the Vf index for five different periods (P1, P2, P3, P4 & P5) of valley formation, developed between five fluvial terraces (P1: T1, T2, T3, T4 & T5; P2: T6, T7, T8, T9 & T10; P3: T11, T12, T13, T14 & T15; P4: T16, T17, T18, T19, & T20; P5: T21, T22, T23, T24 & T25; Figure 9). Next, we related this data to the river incision rates extracted from the Lozoya River terrace sequence (P1≈0.055 mm/a, P2≈0.07 mm/a, P3≈0.065 mm/a, P4≈0.006 mm/a & P5≈0.1 mm/a). In cases where the terraces were not preserved along the cross-section, we interpolated their values from the closest preserved terraces (Benito-Calvo & Pérez-González; 2008). This method allows us to analyze the spatio-temporal incision controlled mainly by bedrock characteristics, uplift processes and climatic conditions (Figure 9; Table 2).

Stream length–gradient Index (SL)

The SL index has been widely used as an xy-profile to identify anomalies in stream profiles (Hack, 1973; Silva *et al.*, 1988; Fernández-García & Garzón Heydt, 1994; Garrote *et al.*, 2002; Garzón Heydt *et al.*, 2012). In this study, we created an SL map using 5-m resolution DEM and GIS, following the method proposed by Font *et al.*, (2010). From the DEM, we extracted a slope percentage map, which was later used to calculate the SL index along the longitudinal profiles of the drainage network. These data were used to interpolate a continuous stream length–gradient surface by applying ordinary kriging (Figure 10).

Longitudinal slope and curvature profile

The longitudinal profiles of streams have always been considered very important data for hydrological and geomorphological studies. The profile convexities are identified as slope changes or escarpments in the streams, and are associated with disequilibrium and non-steady states (Hack, 1973). They are usually correlated with base level lowering, lithological variations, structural trending, sediment inputs, nonfluvial processes and human modifications (Richards, 1982; Knighton, 1998;

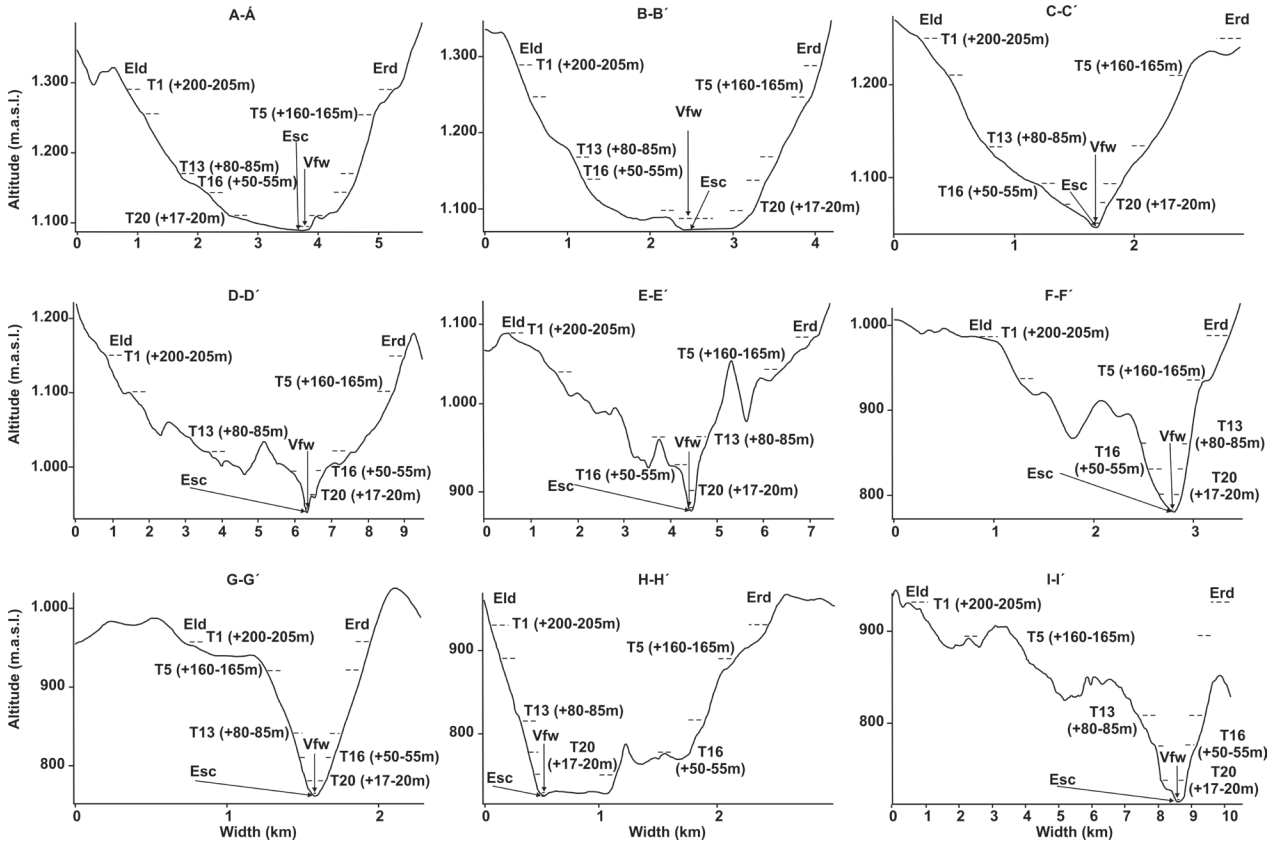

Figure 8.—Geomorphological cross-sections along the Lozoya River valley, used to calculate the Vf index for the five Quaternary periods considered.

Burbank & Anderson, 2001; Schumm, 2005; Gasparini *et al.,* 2007; Phillips & Lutz, 2008; Benito-Calvo *et al.*, 2015). On the other hand, concave-up shapes in longitudinal stream profiles are usually associated with flat and steady-state areas (Leopold, 1994; Sinha & Parker, 1996; Morris & Williams, 1997; Smith *et al.,* 2000; Larue, 2008; Phillips & Lutz, 2008). This assumption is based on stream power theory in that upstream the erosion and slope are increasing while downstream the gradient and discharge energy are decreasing (Smith *et al.,* 2000; Snyder *et al.,* 2000; Roe *et al.,* 2002; Duvall *et al.,* 2004; Goldrick & Bishop, 2007; Phillips & Lutz, 2008). However, we have to be careful with this notion because nonsteady conditions can also produce a smooth concave longitudinal profile (Snow & Slingerland, 1987; Ohmori, 1991; Sinha and Parker, 1996; Whipple, 2004). The analysis of the profile allowed us to identify the major irregularities in the stream longitudinal profile (Figure 11).

The analysis of longitudinal profile irregularities was extended to longitudinal profiles of the Lozoya terraces, to check for the persistence of the anomalies through time (Figures 10 & 11). To do so, the terrace longitudinal profiles were reconstructed using the n^{th} degree polynomial functions (Benito-Calvo *et al.,* 2008), which displayed the best fit ($R^2 > 0.99$). Additionally, to examine whether these knickpoints are pre–Quaternary, we reconstructed the bedrock paleotopography of an extensive and well-preserved Turolian coarse-grained alluvial fan system (Profile G3; Figures 1 & 10; Bellido *et al.,* 1991b; Portero *et al.,* 1990; Karampaglidis *et al.,* 2020). These deposits lie in the Atazar and Ponton de la Oliva sectors, parallel to the Lozoya River and always in the NE part of the modern flow (Figure 1). To reconstruct the paleoprofile we used the contact of the deposits with the Paleozoic basement and Early Miocene sediments as a reference point (Figures 1 & 10).

Concavity Index (CI)

The Concavity Index was used to analyze the general shape of the longitudinal profiles (Table 3). It was computed on the basis of deviations from a straight line (Phillips & Lutz, 2008):

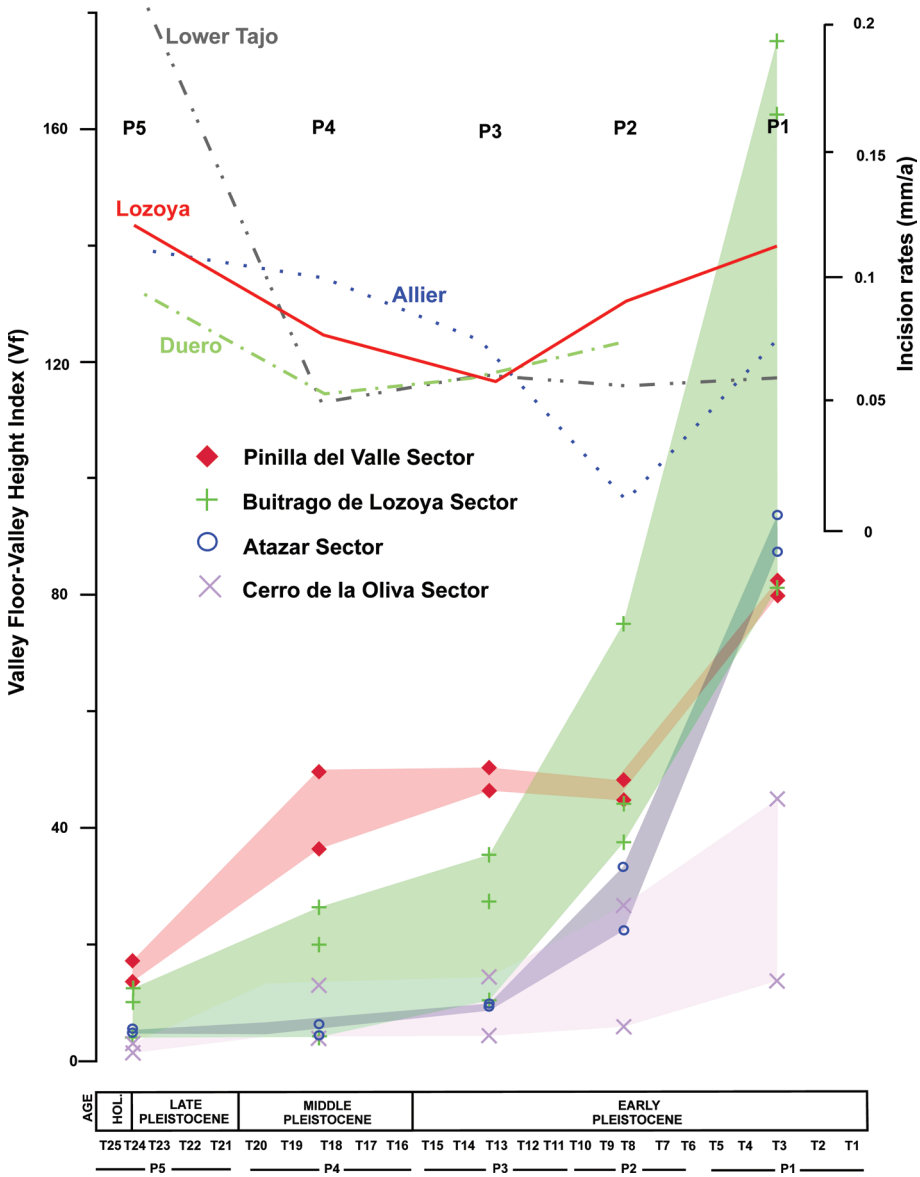

Figure 9.—Evolution of the Vf index through the Quaternary in the four sectors defined in the Lozoya watershed.

$$CI = \Sigma(Hi^*-Hi)/N$$

where Hi is the elevation at distance i, Hi* is the elevation along a straight line from the uppermost to lowermost point along the stream line at horizontal distance i, and N is the total number of measurement points. Negative CI values indicate convexity, whereas positive CI values indicate concavity. Convexities in long profiles are typically associated with base level lowering, litho-structural controls, sediment inputs, nonfluvial erosion processes, bedload fluctuations and human modifications, while smooth concave-up long profiles have long been considered as steady-state equilibrium forms (Phillips & Lutz, 2008).

Results and discussion

The Lozoya watershed has a complex morphology characterized by several incision geometries, which change through time and space. In the Upper and Middle Lozoya watershed (Pinilla del Valle, Buitrago de Lozoya and Atazar sectors), steep slopes are concentrated in the range alignments (Figure 5),

Table 2.—Values of the Vf index estimated for the Lozoya River. See location in Figure 2.

Section	Sector	Period	Terraces	Vfw (m)	Eld (m)	Erd (m)	Vf
A-A´	Lozoya	P1	T1 (+200-205m) - T5 (+160-165m)	3300	40	40	82.5
		P2	T5 (+160-165m) - T11 (+100-104m)	2900	60	60	48.3
		P3	T11 (+100-104m) - T16 (50-55m)	2500	50	50	50.0
		P4	T16 (50-55m) - T20 (+17-20m)	1500	30	30	50.0
		P5	T20 (+17-20m) - Lozoya River	345	20	20	17.3
B-B´	Lozoya	P1	T1 (+200-205m) - T5 (+160-165m)	3200	40	40	80.0
		P2	T5 (+160-165m) - T11 (+100-104m)	2700	60	60	45.0
		P3	T11 (+100-104m) - T16 (50-55m)	2300	50	50	46.0
		P4	T16 (50-55m) - T20 (+17-20m)	1100	30	30	36.7
		P5	T20 (+17-20m) - Lozoya River	275	20	20	13.8
C-C´	Buitrago de Lozoya	P1	T1 (+200-205m) - T5 (+160-165m)	3250	40	40	81.3
		P2	T5 (+160-165m) - T11 (+100-104m)	2250	60	60	37.5
		P3	T11 (+100-104m) - T16 (50-55m)	1350	50	50	27.0
		P4	T16 (50-55m) - T20 (+17-20m)	600	30	30	20.0
		P5	T20 (+17-20m) - Lozoya River	200	20	20	10.0
D-D´	Buitrago de Lozoya	P1	T1 (+200-205m) - T5 (+160-165m)	7000	40	40	175.0
		P2	T5 (+160-165m) - T11 (+100-104m)	4500	60	60	75.0
		P3	T11 (+100-104m) - T16 (50-55m)	1750	50	50	35.0
		P4	T16 (50-55m) - T20 (+17-20m)	800	30	30	26.7
		P5	T20 (+17-20m) - Lozoya River	250	20	20	12.5
E-E´	Buitrago de Lozoya	P1	T1 (+200-205m) - T5 (+160-165m)	6500	40	40	162.5
		P2	T5 (+160-165m) - T11 (+100-104m)	2650	60	60	44.2
		P3	T11 (+100-104m) - T16 (50-55m)	500	50	50	10.0
		P4	T16 (50-55m) - T20 (+17-20m)	125	30	30	4.2
		P5	T20 (+17-20m) - Lozoya River	80	20	20	4.0
F-F´	Atazar	P1	T1 (+200-205m) - T5 (+160-165m)	3750	40	40	93.8
		P2	T5 (+160-165m) - T11 (+100-104m)	2000	60	60	33.3
		P3	T11 (+100-104m) - T16 (50-55m)	470	50	50	9.4
		P4	T16 (50-55m) - T20 (+17-20m)	140	30	30	4.7
		P5	T20 (+17-20m) - Lozoya River	100	20	20	5.0
G-G´	Atazar	P1	T1 (+200-205m) - T5 (+160-165m)	3500	40	40	87.5
		P2	T5 (+160-165m) - T11 (+100-104m)	1350	60	60	22.5
		P3	T11 (+100-104m) - T16 (50-55m)	450	50	50	9.0
		P4	T16 (50-55m) - T20 (+17-20m)	200	30	30	6.7
		P5	T20 (+17-20m) - Lozoya River	100	20	20	5.0
H-H´	Cerro de Oliva	P1	T1 (+200-205m) - T5 (+160-165m)	550	40	40	13.8
		P2	T5 (+160-165m) - T11 (+100-104m)	350	60	60	5.8
		P3	T11 (+100-104m) - T16 (50-55m)	200	50	50	4.0

Continued

Tabla 2.—Continued

Section	Sector	Period	Terraces	Vfw (m)	Eld (m)	Erd (m)	Vf
		P4	T16 (50-55m) - T20 (+17-20m)	125	30	30	4.2
		P5	T20 (+17-20m) - Lozoya River	30	20	20	1.5
I-I´	Cerro de Oliva	P1	T1 (+200-205m) - T5 (+160-165m)	1800	40	40	45.0
		P2	T5 (+160-165m) - T11 (+100-104m)	1600	60	60	26.7
		P3	T11 (+100-104m) - T16 (50-55m)	700	50	50	14.0
		P4	T16 (50-55m) - T20 (+17-20m)	400	30	30	13.3
		P5	T20 (+17-20m) - Lozoya River	60	20	20	3.0

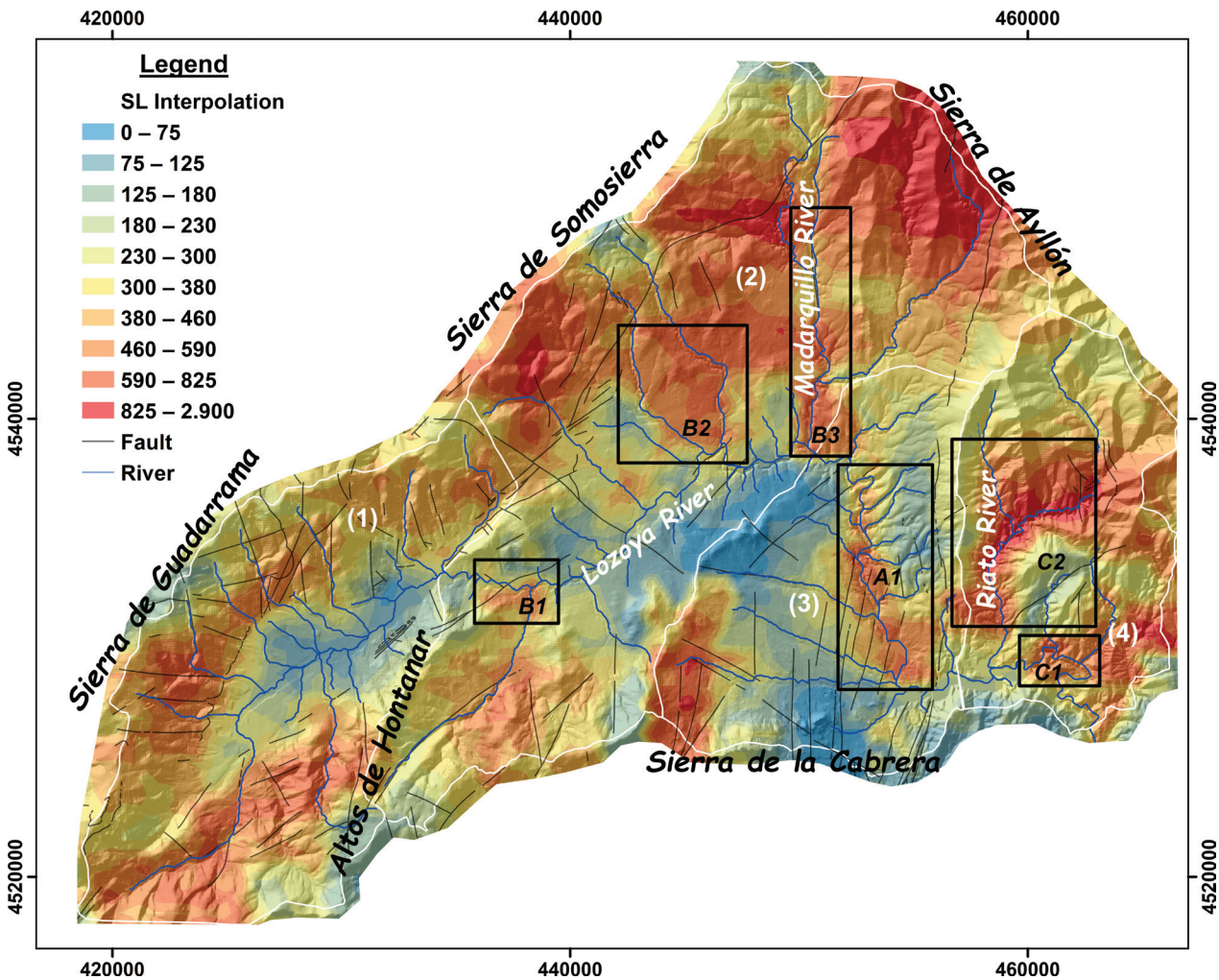

Figure 10.—Stream length–gradient index (SL) map, calculated for the Lozoya River study area. The black lines correspond to the main faults in the study area. The SL values were classified using the quantile method.

while at lower altitudes, smooth landforms formed on orthogneiss and leucogneiss predominate. On the other hand, in the Lower Lozoya watershed (Cerro de la Oliva sector), narrow and incised valleys develop on the paragneiss, schist, black slate and quartzite series, prompting a significant increase in

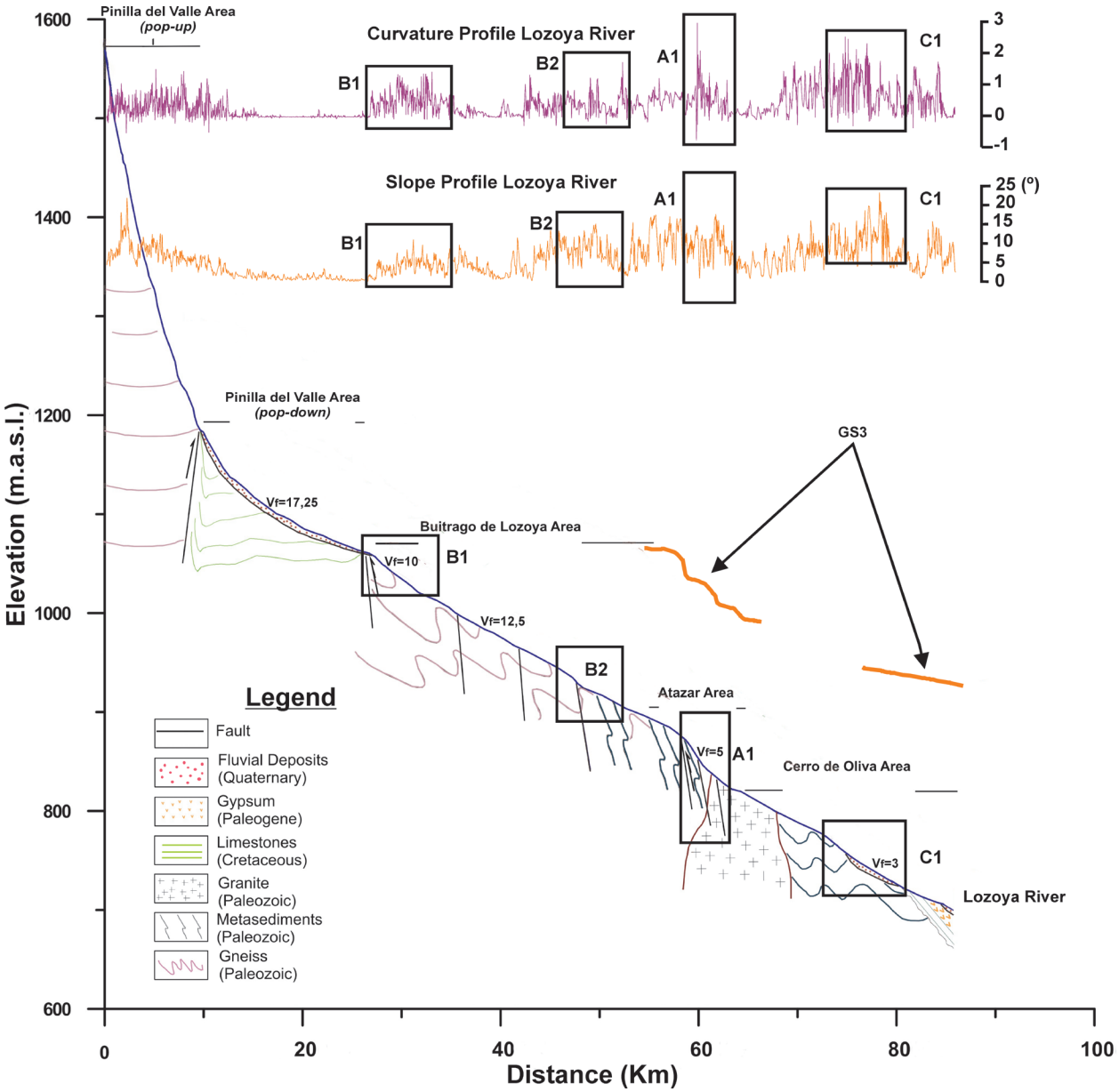

Figure 11.—Lozoya longitudinal profile and identification of the main knickpoints, with the assistance of slope and curvature profiles.

Table 3.—Concavity indices for the entire Loyoza River and within the four sectors identified according to their morphostructural and lithological characteristics.

	Lozoya River	Lozoya Valley Area	Buitrago de Lozoya Area	Atazar Area	Cerro de Oliva Area
CI	153.85	236.9	174	103.5	42.2
CIrel	0.36	0.55	0.4	0.24	0.098

steep slopes (Figure 5; Karampaglidis *et al.,* 2011). The diverse lithology has an important impact on the formation of the local morphological features in each sector, and consequently on the incision of the valleys (Karampaglidis *et al.,* 2014b). Regarding the shape of the Lozoya Valley, the upper part (Pinilla del Valle

sector) is generally U-shaped (profiles A-A′, B-B′ & C-C′; Figure 8), whereas in the downstream sectors (Buitrago de Lozoya, Atazar and Cerro de la Oliva), open valley morphologies are restricted to the earlier development stages (profiles D-D′, E-E′, F-F′, G-G′, H-H′ & I-I′; Figure 8). Subsequent stages in these sectors generate narrow valleys, with different sinuosities, where vertical incision and entrenchment predominate.

Transverse topographic asymmetry factor (T-index) analysis

The origin of asymmetric basins could be associated with lithological-structural variation and/or tectonic activity. The T-index is effective for highlighting tilted areas (Garrote *et al*., 2008). In our case, the transverse topographic asymmetry values display a clear spatial distribution (Figure 5). Small to medium magnitudes are identified in the Pinilla del Valle and Buitrago de Lozoya areas with three prominent directions of river migration: SW, NW and SE. On the other hand, in the Atazar area the T-index values are higher, between 0.3 and 0.5, with only one prominent migration direction (E). Finally, the highest values (>0.5) are identified in the Ponton de la Oliva area, with north and east lateral migrations of the river direction (Figure 5).

In the case of the high asymmetry values in the Atazar area, no geological evidence of neotectonic activity on the preserved Turolian sediments or on the Quaternary landforms has been identified (Portero *et al., 1990*; Bellido *et al.,* 1991a; Andeweg *et al.,* 1999; Karampaglidis, 2015). Probably, the high values are related to lithological changes delimited by the Lozoya River, located between gentle western slopes on Permian granites and rugged terrain developed on Paleozoic metasediments on the eastern side (Figure 1 & 4). This is a very common feature in the MCB (Garrote *et al.,* 2008), where Miocene detrital sedimentary rocks with extended terraces are located on the western margin, whereas gypsum escarpments characterize the eastern margin (Silva *et al.,* 1988). Pontón de la Oliva is the other sector with high values. In this case the lithology is homogeneous (Figure 1) and high T values cannot be explained by bedrock lithological changes. Just as in the previous sector, the left margins of the Lozoya River are characterized by Turolian detrital sediments with no tectonic evidence of large block tilting (Portero *et al.,* 1990; Bellido *et al.,* 1991a; Andeweg *et al.,* 1999; Karampaglidis, 2015). In the MCB, Garrote et al., 2008 have related the basin asymmetry of the Jarama, Henares, Tajuña and Tajo rivers to the principal morpho-structural patterns of the basin, influenced by the crustal undulations previously defined for the basin. At this point, it is worth mentioning that this area stands out for the Atazar and Tortuero backthrust structures with N-S trend and left-lateral strike-slip movement up to the Somosierra Pass Fault (Figures 1 & 4; Vicente *et al.,* 2007). The Lozoya River general trend in this area is ENE, downcutting parallel to the Atazar backthrust structure, which is a relatively depressed area and almost perpendicular to the NNE direction of the center of the Madrid basin (Figures 1 & 4). Similarly, to Garrote et al., 2008, we can attribute the high T values to previous morpho-structural trends in response to Alpine tectonics and to the old Lozoya River capture (Karampaglidis *et al.,* 2011). The latter would have produced a reorganization of the local drainage in this sector. The stream capture of an asymmetric basin could lead to an acceleration of the river's incision without external forcings (Prince *et al.,* 2011) and when entrenchment continued, the Lozoya River would have incised and captured the local streams running SW, the same direction as the center of the MCB (Figures 2(b) & 4) (Karampaglidis *et al.,* 2011).

Incision rates and valley width to valley height ratio index analysis

The incision rates and Vf index are very useful tools for detecting areas with base level lowering. In order to analyze the temporal and spatial variations, both vertically and horizontally, of the Lozoya valley, first of all, we calculated incision rates for the whole basin during the five different periods (P1, P2, P3, P4 & P5) and secondly, we applied the Vf index in the different sectors and to different stages (P1, P2, P3, P4 & P5) of the valley development (Figure 8; Table 2). The incision rates vary from 0.06 to 0.1 mm/a and two periods of high acceleration are the first thing we notice (Figure 9; Table 4). For the Vf index the lowest values (close to 0) are located from

Table 4.—Incision rate values, estimated for the Lozoya, Lower Tajo, Upper Tajo, Duero and Allier rivers.

Author	River	Name in this work	Age (Ma)	Incision rates mm/a
Cunha et al., 2008	Lower Tajo River	P5	0,1-	0.600
		P4	0,78-0,1	0.060
		P3	1,5-0,78	0.058
		P2	1,95-1,5	0.063
		P1	2,58-1,95	0.060
Pastre 2005	Allier River	P5	0,1-	0.115
		P4	0,78-0,1	0.100
		P3	1,5-0,78	0.075
		P2	1,95-1,5	0.009
		P1	2,58-1,95	0.075
Silva et al., 2017	Duero River	P5	0,1-	0.093
		P4	0,78-0,1	0.057
		P3	1,5-0,78	0.067
		P2	1,95-1,5	0.073
		P1	2,58-1,95	
This work	Lozoya River	P5	0,1-	0.175
		P4	0,78-0,1	0.080
		P3	1,5-0,78	0.060
		P2	1,95-1,5	0.090
		P1	2,58-1,95	0.154

the D-D' to I-I' cross-sections. In these areas the valley shape is asymmetrical and steep (Figures 2(a) & 7). Overall, the Lozoya valley shows a general tendency to develop a more pronounced V-shaped geometry with time. This is an obvious behavior in a downcutting staircase valley, where uplift processes are accepted as triggering incision and as generating the differences in height between fluvial levels (Westaway *et al.,* 2009).

This estimation of the incision rates dynamic during the Quaternary permitted us to compare the long-term incision rates of the Lozoya River with other studies of staircase fluvial sequences such as: Duero (Central-North Spain; Silva *et al.,* 2017; Rodríguez-Rodríguez *et al*., 2020), Upper-Lower Tajo (Central-South Spain; Cunha *et al.,* 2008; Pérez-González 1994; Silva *et al*., 2017; Karampaglidis *et al.,* 2020) and Allier (Central-North France; Pastre 2005). For P1 up to P2, the Lozoya River shows high incision rates (0.15 mm/a) and a large Vf index, between 180 and 80. The highest values of Vf are located in the Buitrago de Lozoya and Atazar areas. Similar incision rates for this period have identified for the Jarama River extended alluvial plains (~0.15 mm/a) and related with climatic changes and the capture of the MCB from the Atlantic drainage system (Karampaglidis *et al.,* 2020). This anomaly is not detected for the Lower Tajo basin (Figure 9). For this period, extended erosive plains have been identified in the Buitrago de Lozoya and Atazar areas (Karampaglidis *et al.,* 2014a). This probably explain the high values of Vf at the start of the P1 period. For the periods P2 and P3, the higher Vf values are identified in the Buitrago de Lozoya area, between 80 and 20, while the lower ones are in the Ponton de la Oliva area, between 20 and 5 (Figure 9). In this period, the Buitrago de Lozoya and Atazar areas are still asymmetric, while the Ponton de la Oliva sector is characterized by steep valleys (Figure 8). Asymmetries and steep valleys, applying the Vf index, are also observed in the Duero basin on the metamorphic rocks and granites and attributed to

lithological variability and drainage capture (Antón *et al*., 2014). During these periods, valleys are still steepening, while the incision rates are falling from 0.09 mm/a to 0.06 mm/a (Figure 9). This indicates no abrupt changes in incision rate. For these periods, this trend has been identified in other large tectonically quiescent Atlantic drainage basins such as the Duero (Central-North Spain), Upper-Lower Tajo (Central-South Spain) and Allier (Central-North France) with values ranging between 0.05 and 0.075 mm/a (Figure 9; Table 4). Finally, for P4 and P5 an acceleration of the incision rates up to 0.175 mm/a has been detected and coincides with the falling trend in Vf (Figure 9). During these periods, the Buitrago de Lozoya, Atazar and Ponton de la Oliva areas are attaining maximum valley steepness (Figure 8). We can easily observe the same trend in the other basins, with the Duero and Allier basins at 0.1 mm/a and 0.115 mm/a respectively. Silva *et al.,* 2017 related this phenomenon with Middle Pleistocene transition driven by climatic fluctuations. For the Lower Tajo basin, the same pattern is repeated but with a much more dynamic rise in values (up to 0.6 mm/a). Cunha *et al.,* 2008 suggested that these high values are driven by an episode of crustal uplift while Silva *et al.,* 2017 proposes eustatically forced controls.

However, not all the sectors show exactly the same dynamic: the Vf curve in the Upper Lozoya Valley (Pinilla del Valle sector, Figure 9) shows a different pattern for the periods P2 and P4. Vf values are stable and stand between 50 and 40. Most likely, the pop-down NE-SW morphology of the SCS crystalline basement, delimited by lithological contrast between Paleozoic gneisses and Cretaceous dolomites to the south and Paleozoic gneisses with Tertiary detrital sediments to the north (Figure 1) maintained stable shape ratios from the Early Pleistocene (P2) to the Middle Pleistocene (P4). The lithological contrast between high rock strength gneisses with highly soluble and fractured limestones and low strength sediments probably favors valley opening, lateral planation and smoothing from weathering and erosion. Schanz & Montgomery, 2016 observed that slaking weathering and crystalline transported material as bedload over weaker sedimentary units acts as an abrasion tool and foments rapid valley widening. Seen in this light, the widening of the valley could generate large values for Vfw, and this keeps Vf stable and yields a U-shape effect. During the Middle Pleistocene an extended karstic system developed on the local Cretaceous dolomites which could foster this (Pérez-González *et al.,* 2010). Subsequently, in the Upper Pleistocene (P5), the valley shape changed sharply, coinciding with the development of the youngest strath terrace and small alluvial fans. In this case, Vf presents the same dynamic as in the other sectors.

Longitudinal profile analysis

The interpretation of the Vf and T-index values was combined with the information provided by the stream longitudinal profile analysis. The SL index represents the slope variation along the stream profiles (Hack, 1973; Font *et al.,* 2010). Whereas high values are normally located in upstream areas and could perfectly well be related to drastic changes in relief due to erosion, further downstream, they are very commonly associated with knickpoint areas (Hack, 1973; Garrote *et al.*, 2002; Pérez-Peña *et al.,* 2009; Font *et al.,* 2010; Garzón Heydt *et al.*, 2012; Antón *et al.,* 2014; Soria-Jauregui *et al.,* 2018). In the MCB, Silva *et al.,* 1988 related high SL values for the Jarama and Manzanares rivers with bedrock variability and neotectonic activity associated to halokinetic and subkarst dissolution processes of the bedrock, together with the reactivation of large basement faults. Other authors such as Pérez-Peña *et al.,* 2009 demonstrate that in the Granada Basin, high SL values could be related to the large drainage areas, while in the Duero Basin, Antón *et al.* (2014) attribute them to drainage reorganization prompted by the capture of the endorheic basin from the exorheic Atlantic drainage system. In the present study, the stream length–gradient index (SL) was calculated including the main stream profiles of the Lozoya watershed, interpolating to create a map for the entire study area (Figure 10). This map shows certain zones in the lower part of the Lozoya valley with high SL values (Figure 10). The first anomalous zone (B1; Figure 10), defined by intermediate SL values, was where the Lozoya River abandoned the upper valley pop-down depression, cutting a NE-SW structural alignment (profile C-C´; Figure 8). In this case it seems to

be influenced by the Alpine structure trends and bedrock lithological contrast between Cretaceous limestones and Paleozoic gneisses (Figure 1& 10). Towards the north, Lozoya tributaries have high SL values (zones B2 and B3) coinciding with canyons incised following a N-S band of schist and slates in structural contact with gneisses (Figure 1). Bedrock lithology contrast and structural contact between metasediments and metaplutonic rocks can generate weakened bedrock areas with differing response to erosion by local streams (Antón *et al*., 2014). In the Atazar sector, the SL index allowed us to distinguish a large zone with steep gradients along the Lozoya canyon carved into the lithological-structural contact between the orthogneisses and leucogneisses, and fractured metasediments and granites (zone A1, Figures 1 & 9). Below the Atazar Dam (Cerro de la Oliva sector), the Lozoya River again shows high SL values (zone C1). This coincides with the elbow capture where the old Lozoya tributaries and the Lozoya River were captured (Karampaglidis *et al*., 2011), causing an increase in gradient here and adjustment of the tributaries to the new base level (zone C2; Figure 10). As we can observe, the SL index is a powerful tool for identifying topographical breaks along a stream (knickpoints), but further considerations are needed to interpret it.

Recognition of the most representative anomalies was facilitated by analysis of the slope and curvature variability along the Lozoya longitudinal profile (Figure 11). The current Lozoya longitudinal profile shows the normal tendency to decrease in concavity downstream (Table 3), although with several anomalies. The headwater of the Lozoya River has several minor irregularities, shown by a high variability in the slope and curvature profiles. This variability profile decreases sharply in the pop-down Pinilla del Valle depression, and rises again in the Middle and Lower Lozoya Valley (Buitrago de Lozoya, Atazar and Cerro de la Oliva sectors). Within these sectors, slope and curvature profiles show several major knickpoints, which coincide with the high SL zones detected for the Lozoya River and its entrenchments (zones B1, B2, A1 & C1; Figure 10 & 11). Some of these knickpoints appear related to faults (B1, B2 & A1), and differential uplift associated with Quaternary fault reactivation could be suggested. To assess this point, we analyzed the persistence of these knickpoints over time, by reconstructing the longitudinal profiles of the Lozoya terraces and the paleotopography where the Turolian detrital sediments have been deposited (Figures 10 & 11). Data from terraces have coarser resolution than the modern Lozoya longitudinal profile, but the trend of the terrace profiles and the terrace height data were useful in providing insights into the persistence of the major knickpoints during the downcutting process. The convex morphology of the B1 knickpoint can be recognized in the terrace profiles developed from the Lower-Middle Pleistocene to the present day (T13-T24), whereas earlier terrace profiles do not provide clear evidence to support the existence of this knickpoint. Nevertheless, the straight or concave morphologies shown by the oldest terrace profiles in the B1 zone might be artifacts of the limited data available to interpolate the oldest terraces. This situation is similar for the knickpoint A1, easily identifiable in terrace profiles T13-T24, but with a very weak signal in older terraces. For example, in terrace profiles T2-T5, the general trend of the interpolated curve does not reflect knickpoint A1, yet it can be recognized in the local data shown by the terrace heights (Figure 12). Further, the reconstructed GS3 profile suggests that the presence of the A1 main trend is clearly pre-Quaternary, since at least the Turolian, and the Lozoya River is smoothing it out (Figure 11). In addition, it should be noted that there is no evidence of postfaulting or dipping for these deposits (Portero *et al.,* 1990; Bellido *et al.,* 1991a; Andeweg *et al.* 1999; Karampaglidis, 2015). This could suggest that the A1 knickpoint origin is related to a response to Alpine tectonics and/or neotectonic reactivation from Late Miocene active thrusting, whereas the southern border of the SCS was covered by Turolian sediments (Andeweg *et al.* 1999; Vicente *et al.,* 2007; Karampaglidis *et al.,* 2020).

Analysis of the stream longitudinal profiles indicates that the main knickpoints detected have an Alpine origin associated with the trends of the SCS principal structures in this area and controlled by lithological contrast and stream capture. Additionally, reconstructions of terrace profiles show no significant differential movements associated with fault reactivation from at

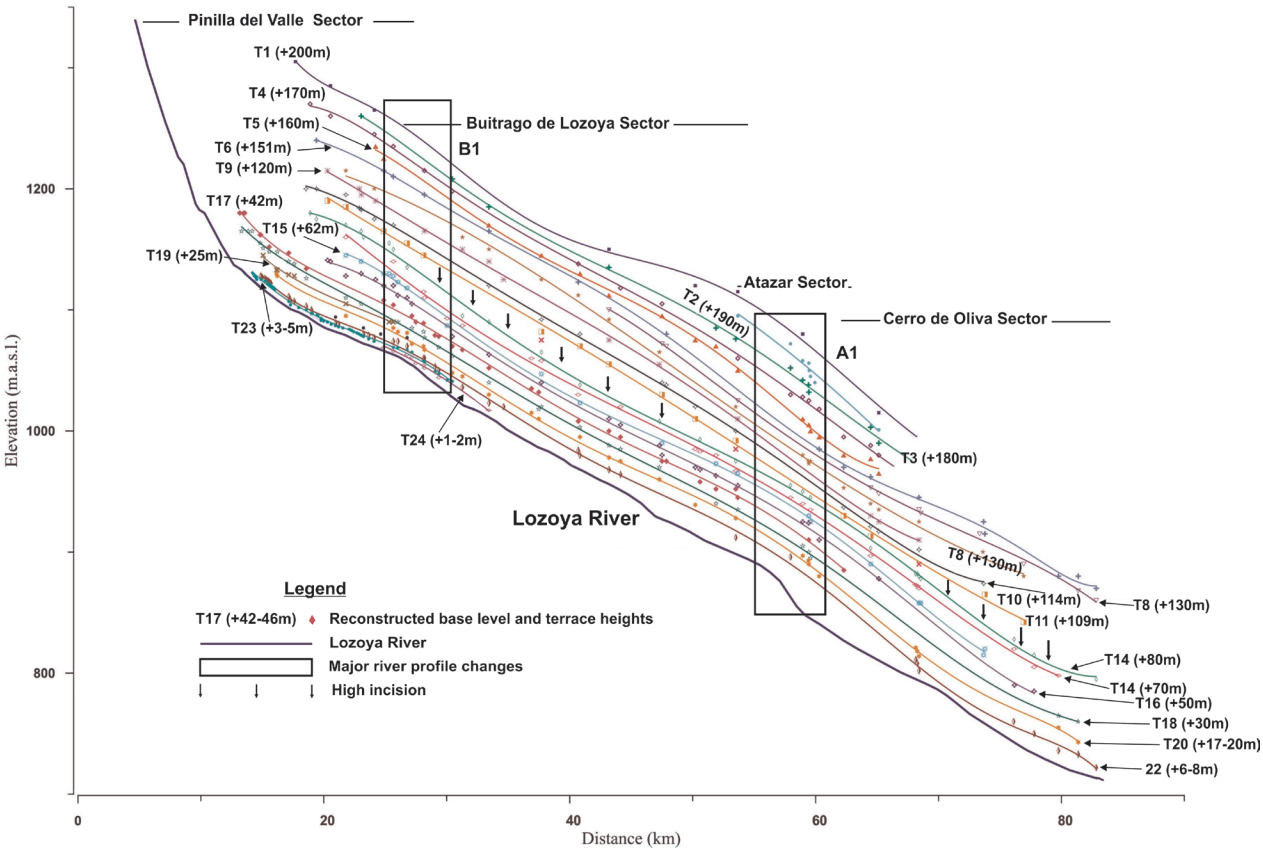

Figure 12.—Evolution of the Lozoya longitudinal profile during the Quaternary, using the reconstruction of the longitudinal profiles for the terrace sequence.

least the Early-Middle Pleistocene boundary to the present day.

Lithological–morphostuctural controls for Lozoya bedrock terrace formation and preservation?

Combining the Lozoya terrace records and geomorphometric indices we observe that the Lozoya drainage basin evolution seems to be conditioned by Alpine morphostructural trends, lithological contrast, river captures assessed both at the local and basin level, climatic fluctuations and denudational uplift. Thus, at this point the mix of these patterns could explain the Lozoya basin's erosive staircase style and the poor preservation of the terrace alluvial cover in some sectors. The shape, size and preservation of bedrock terraces depend on: climatic variations which configure sediment supply and river discharge (Hancock & Anderson, 2002; Turowski *et al.,* 2007, 2008; Yanites & Tucker, 2010); base level lowering caused by sea level changes or tectonics (Merritts *et al.,* 1994) or river capture (Stokes *et al.,* 2017); lithological contrasts (Schanz & Montgomery, 2016; Stokes *et al.,* 2017) and internal forcings such as meander cutoffs (Finnegan & Dietrich, 2011).

In the Lozoya drainage basin, a long staircase sequence was identified (24 levels), with 15 Early Pleistocene, 5 Middle Pleistocene and 4 Late Pleistocene levels (Karampaglidis *et al.,* 2014a). The vertical separation between the terraces is ~10-15 m for the Early Pleistocene ones, while for the Middle-Late ones it is lower: ~3-7 m. The sequence is mainly composed of strath and bedrock terraces. Bedrock, or strath, river terraces are formed when there is a change in ratio from vertical incision to lateral erosion (Hancock & Anderson, 2002). When rivers with an alluvial cover migrate across valley bottoms, the underlying bedrock is eroded into a planar surface called a strath (Personius *et al.,* 1993; Wegmann & Pazzaglia, 2002; Fuller *et al.,* 2009;

Finnegan & Balco, 2013; Pazzaglia, 2013; Schanz & Montgomery; 2016). In the Buitrago de Lozoya and Atazar areas, the river cut through Paleozoic gneisses and granites, and the identified terraces are mainly erosive, with poor preservation of the alluvial cover. Meanwhile, in the Upper Lozoya and Ponton de la Oliva sectors strath terraces 2-4 m thick are recognized, with massive structure and oligomictic material. In these sectors, the Lozoya River cuts through Cretaceous dolomites or Miocene detritals sediments and black slates respectively. So, it is obvious that the bedrock geology influenced the preservation of the alluvial cover. Indeed, this is very common: Montgomery (2004) observed that alluvial cover formation and/or preservation is easier on less resistant lithologies like sandstone and siltstone than more resistant ones such as quartzite and basalt. Along the same lines, Stokes *et al.* (2017) contend that underlying bedrock geology and its stratigraphic and structural configuration play a role just as important as other mechanisms (lowering and climate) in terrace formation and/or preservation. Furthermore, Schanz & Montgomery (2016) showed that bedrock lithology is a very important factor in the rates of lateral erosion influencing floodplain width and the potential for bedrock planation and bedrock cover preservation. In the same study, they notice the importance of physical weathering from wetting and drying in alluvial cover preservation. In our case, in the Atazar and Buitrago de Lozoya sectors, the Paleozoic granites and gneisses bedrock has a high mica content and is prone to physical weathering (Bellido *et al.,* 1991b; Karampaglidis *et al.,* 2014a). In addition, as we have seen, in these areas we identified three pre-Quaternary knickpoints (A1, B1 & B2; Figure 10) which break the Lozoya River's longitudinal profile abruptly and thus produce acceleration and higher stream power, so that stronger vertical incision could take place locally. In addition, Schanz & Montgomery (2016) observed that strong vertical incision creates erosive point banks perched above the water table and exposed to mechanical and chemical weathering processes. That means that on rocks prone to weathering during high flows with crystalline bedload, the weathered material is rapidly washed away, perhaps resulting in centimeters of lateral erosion in a single event (Montgomery, 2004; Stock *et al.,* 2005; Collins *et al.,* 2016). Thus, fast-weathering lithology with existing morphostructural longitudinal profile anomalies could explain the poor preservation of the alluvial bedrock cover in these areas. At this point it should be mentioned that more research along these lines is needed, and a detailed study of erosion rates and surface dating will probably help us improve our understanding.

Conclusions

Combining morphometric indices in the Lozoya watershed and using the topography of identified past geomorphic base levels proves to be a useful method for characterizing the incision shapes and understanding the lithological, geomorphic and climatic controls during the evolution of the Quaternary valley. In summary, the study shows:

1. The main Lozoya River trends seem to be conditioned by the previous morphostructure of the principal Alpine structures in this area: the NE-SW pop-down in the Upper Lozoya sector, ENE-WSW Guadarrama pop-up in the Buitrago de Lozoya sector, the lithostructural contact with N-S trend in the Atazar sector and the Atazar backthrust with N-S trends in the Ponton de la Oliva sector.
2. The principal breakdown areas in the Lozoya longitudinal profile in the Buitrago de Lozoya and Atazar sectors are related with Alpine structures and lithological contrast. These knickpoints are identified in the reconstructed profiles of the Lozoya River fluvial terraces and in the bedrock paleotopography of an extended and well-preserved Turolian coarse-grained alluvial fan system. The reconstructed profiles do not show Quaternary fault reactivation.
3. Spatial and temporal analysis of the Vf index and incision rates permitted us to model the Lozoya River's dynamic over time. Vf values and incision rate acceleration in the Early Pleistocene are related to the MCB capture from the Atlantic drainage system, while the Middle-Late Pleistocene acceleration is associated with climatic changes.
4. The low rock strength of Cretaceous dolomites eroded by crystalline bedload transported by local drainage can produce rapid valley widening.

5. Bedrock lithology and previous morphostructure can explain the poor preservation of the bedrock cover of the Lozoya River terraces.
6. Morphometric indices are a very useful tool for understanding the principal formation mechanisms of the landscape but it is highly recommended to follow this up by detailed geomorphological analysis.

ACKNOWLEDGMENTS

This work was funded by the Research Project of the Archaeological Sites of the Pinilla del Valle (Comunidad Autónoma de Madrid, Spain). We would like to thank Francisco Gutiérrez for his useful suggestions and comments that improved the consistency and clarity of the manuscript. The authors are also grateful to George Patsiaouras and Colin Woodham for their careful revision of the text.

References

Alonso-Zarza, A.M.; Calvo, J.P. & Garcia del Cura, M.A. (1993). Palaeogeomorphological controls on the distribution and sedimentary styles of alluvial systems, Neogene of the NE of the Madrid Basin (central Spain). Special Publication of the International Association of Sedimentologists, 17: 277-292.

Andeweg, B.; Vicente, G. De; Cloetingh, S.; Giner, J. & Muñoz Martin, A. (1999). Local stress fields and intraplate deformation of Iberia: variations in spatial and temporal interplay of regional stress sources. Tectonophysics, 305: 153-164. https://doi.org/10.1016/S0040-1951(99)00004-9

Antoine, P.; Lautridou, J.P. & Laurent, M. (2000). Long-term fluvial archives in NW France: response of the Seine and Somme rivers to tectonic movements, climate variations and sea-level changes. Geomorphology 33: 183-207. https://doi.org/10.1016/S0169-555X(99)00122-1

Antón, L.; Rodés, A.; Vicente, G. De; Pallàs, R.; Garcia-Castellanos, D.; Stuart, F.M.; Braucher, R. & Bourlès, D. (2012). Quantification of fluvial incision in the Duero Basin (NW Iberia) from longitudinal profile analysis and terrestrial cosmogenic nuclide concentrations. Geomorphology 165-166: 50-61. https://doi.org/10.1016/j.geomorph.2011.12.036

Antón, L.; De Vicente, G.; Muñoz-Martín, A. & Stokes, M. (2014). Using river long profiles and geomorphic indices to evaluate the geomorphological signature of continental scale drainage capture, Duero basin (NW Iberia). Geomorphology, 206: 250-261.

Arenas, R.; Fúster, J.M.; Martínez, J.; Del Olmo, A. & Villaseca, E. (1991). Mapa Geológico de España a E.1:50.000, Segovia (483). Madrid, IGME.

Arsuaga, J.L.; Baquedano, E. & Pérez-González, A. (2006). Neanderthal and carnivore occupations in Pinilla del Valle sites (Comunity of Madrid, Spain). Proceedings of the XVISPP Congress, British Archaeological Reports, Lisbon 2006.

Aznar, J.M.; Pérez-González, A. & Portero García, J.M. (1995). Mapa Geológico de España a E. 1:50.000, Valdepeñas de la Sierra (485). Madrid, IGME.

Azor, A.; Casquet, C.; Martin, L.M.; Navidad, M.; Del Olmo, A.; Peinado Moreno, M.; Pineda, A.; Villar Alonso, P. & Villaseca, C. (1991). Mapa Geológico de España a E.1:50.000, Prádena (458). Madrid, IGME.

Baena-Perez, J.; Moreno-Serrano, F.; Nozal-Martin, F.; Alfaro-Zubero, J.A. & Barranco-Sanz, L.M. (1998). Mapa neotectónico de España. Madrid, IGME.

Bellido, F.; Casquet, C.; Fúster, J.M.; González, F.; Martin, L.M.; Martínez-Salinova, J. & Del Olmo, A. (2004). Mapa Geológico de España a E. 1:50.000, Torrelaguna (509). Madrid, IGME.

Bellido, F.; Casquet, C.; Fúster, J.M.; Martin, A.; Del Olmo, A. & De Pablo, J.G. (1991a). Mapa Geológico de España a E. 1:50.000, Cercedilla (508). Madrid, IGME.

Bellido, F.; Escuder, J.; Klein, E. & Del Olmo, A. (1991b). Mapa Geológico de España a E. 1:50.000, Buitrago de Lozoya (484). IGME, Madrid.

Benito, A.; Pérez-González, A. & Santonja, M. (1998). Terrazas rocosas, aluviales y travertínicas del valle alto del río Henares (Guadalajara, España). Geogaceta, 24: 55-58.

Benito-Calvo, A.; Ortega, A.I.; Pérez-González, A.; Campaña, I.; Bermúdez De Castro, J.M. & Carbonell, E. (2015). Palaeogeographical reconstruction of the Pleistocene sites in the Sierra the Atapuerca (Burgos, Spain). Quaternary international, 433(A): 379-392. http://doi.org/10.1016/j.quaint.2015.10.034.

Benito-Calvo, A. & Pérez-González, A. (2010). Las superficies de erosión neógenas en la zona de transición entre la Cordillera Ibérica y el Sistema Central (Guadalajara, España). Revista de la Sociedad Geológica de España, 23 (3-4), 145-156.

Benito-Calvo, A.; Pérez-González, A. & Parés, J.M. (2008). Quantitative reconstruction of late Cenozoic landscapes: a case study in the Sierra de Atapuerca (Burgos, Spain). Earth Surface Processes and Landforms, 33: 196-208. https://doi.org/10.1002/esp.1534

Birot, P. & Solé Sabarís, L. (1954). Investigaciones sobremorfología de la cordillera central Española. Instituto Juan Sebastián Elcano, C.S.I.C.; Madrid.

Bishop, P., (2007). Long-term landscape evolution: linking tectonics and surface processes. Earth Surface Processes and Landforms 32: 329-365. https://doi.org/10.1002/esp.1493

Bridgland, D.R. (2000). River terrace systems in north-west Europe: an archive of environmental change, uplift and early human occupation. Quaternary Science Reviews 19, 1293-1303. https://doi.org/10.1016/S0277-3791(99)00095-5

Bridgland, D. & Westaway, R. (2008). Climatically controlled river terrace staircases: A worldwide Quaternary phenomenon. Geomorphology, 98(3-4): 285-315. https://doi.org/10.1016/j.geomorph.2006.12.032.

Bull, W.B. (1978). Geomorphic Tectonic Classes of the South Front of the San Gabriel Mountains, California U.S. Geological Survey Contract Report, 14-08-001-G-394, Office of Earthquakes, Volcanoes and Engineering, Menlo Park, CA.

Bull, W.B. & McFadden, L.D. (1977). Tectonic geomorphology north and south of the Garlock Fault, California. In: Geomorphology in Arid Regions (Doehring, D.O., Ed.). Proceedings Volume of the Eighth Annual Geomorphology Symposium Held at the State University of New York, Binghamton, 115-138. https://doi.org/10.4324/9780429299230-5

Bull, W.B. (2007). Tectonic Geomorphology of Mountains: A New Approach to Paleoseismology. Wiley-Blackwell, Oxford, UK, 326 pp.

Burbank, D.W. & Anderson, R.S. (2001). Tectonic Geomorphology. Oxford: Blackwell. 460 pp.

Capote, R. & Fernández, M.J. (1975). Las series anteordovícicas del Sistema Central. Boletin Geologico y Minero, 86 (6): 551-596.

Capote, R.; González, J.M. & Vicente, G. De (1987). Análisis poblacional de la fracturación tardihercínica en el Sector Central del Sistema Central Ibérico. Cuadernos Do Laboratorio Xeoloxico De Laxe, 11: 305-314.

Carrasco, R.M.; Pedraza, J.; Willenbring, J.K.; Karampaglidis, T.; Soteres, R.L. & Martín-Duque, J.F. (2016). Morfología glaciar del Macizo de Los Pelados-El Nevero (Parque Nacional de la Sierra de Guadarrama). Nueva interpretación y cronología. Boletín de la Real Sociedad Española de Historia Natural Sección Geología, 110: 49-66.

Collins, B.D.; Montgomery, D.R.; Schanz, S.A. & Larsen, I.J. (2016). Rates and mechanisms of bedrock incision and strath terrace formation in a forested catchment, Cascade Range, Washington. Geological Society of America Bulletin, B31340, http://doi.org/10.1130/ B31340.1

Cox, R.T. (1994). Analysis of drainage-basin symmetry as a rapid technique to identify areas of possible Quaternary tilt-block tectonics: an example from the Mississippi Embayment. Geological Society of America Bulletin, 106 (1994): 571-581 https://doi.org/10.1130/0016-7606(1994)106<0571:AODBSA>2.3.CO;2

Cunha, P.; Martins, A.; Huot, S.; Murray, A. & Raposo, L. (2008). Dating the Tejo River lower terraces (Rodao, Portugal) to assess the role of tectonics and uplift. Geomorphology 102, 43-54. https://doi.org/10.1016/j.geomorph.2007.05.019

Cunha, P.P.; Martins, A.A.; Gomes, A.; Stokes, M.; Cabral, J.; Lopes, F.C.; Pereira, D.; Vicente, G. De; Buylaert, J.P.; Murray, A.S. & Antón, L. (2019). Mechanisms and age estimates of continental-scale endorheic to exorheic drainage transition: Douro River, Western Iberia. Global and Planetary Change, 181: 102985. https://doi.org/10.1016/j.gloplacha.2019.102985.

De Bruijne, C.; H. & Andrienssen, P. (2002). Far field effects of Alpine plate tectonism in the Iberian microplate recorded by fault related denudation in the Spanish Central System. Tectonophysics, 349: 161-184. https://doi.org/10.1016/S0040-1951(02)00052-5

Duvall, A.; Kirby, E. & Burbank, D. (2004). Tectonic and lithologic controls on bed-rock channel profiles and processes in coastal California. Journal of Geophysical Research-Earth Surface 109, F03002. doi:10.1029/2003JF000086.

Fernández García, P. & Garzón Heydt, G. (1994). Ajustes en la red de drenaje y morfoestructura en los ríos de Centro-Sur de la cuenca del Duero. In: Geomorfología en España (Arnáez, J. Eds.). Sociedad de Geomorfología, Logroño, 471-484.

Finnegan, N.J. & Dietrich, W.E. (2011). Episodic bedrock strath terrace formation due to meander migration and cutoff. Geology 39: 143-146. http://doi.org/10.1130/G31716. 1.

Finnegan, N.J. & Balco, G. (2013). Sediment supply, base level, braiding, and bedrock river terrace formation: Arroyo Seco, California, USA. Geological Society of America Bulletin, 125: 1114-1124. http://dx.doi.org/10.1130/B30727

Font, M.; Amorese, D. & Lagarde, J.L. (2010). DEM and GIS analysis of the stream gradient index to evaluate effects of tectonics: The Normandy intraplate area (NW France). Geomorphology, 119: 172-180. https://doi.org/10.1016/j.geomorph.2010.03.017

Fuller, T.K.; Perg, L.A.; Willenbring, J.K. & Lepper, K. (2009). Field evidence for climate-driven changes in sediment supply leading to strath terrace formation. Geology, 37: 467-470. http://doi.org/10.1130/G25487A.1.

García-Castellanos, D. & Larrasoaña, J.C. (2015). Quantifying the post-tectonic topographic evolution of closed basins: the Ebro basin (northeast Iberia). Geology, 43: 663-666. https://doi.org/10.1130/G36673.1

Garcia-Castellanos, D.; Verges, J.; Gaspar-Escribano, J. & Cloetingh, S. (2003). Interplay between the tectonics, climate, and fluvial transport during the Cenozoic evolution of the Ebro Basin (NE Iberia). Journal of Geophysical Research, 108(B7). https://doi.org/10.1029/2002JB002073

Garrote, J.; Fernández García, P. & Garzón Heydt, G. (2002). Parámetros morfométricos de la red de drenaje y sus implicaciones estructurales en la cuenca del Tajo. In: Aportaciones a la geomorfología de España en el inicio del Tercer Milenio (Pérez-González, A.; Vegas, J. & Machado, M.J., Eds.). IGME, Madrid, 45-52.

Garrote, J.; Garzón Heydt, G. & Cox, T. (2008). Multistream order analyses in basin asymmetry: A tool

to discriminate the influence of neotectonics in fluvial landscape development (Madrid Basin, Central Spain). Geomorphology, 102: 130-144. https://doi.org/10.1016/j.geomorph.2007.07.023

Garzón Heydt, M.G. (1980). Estudio geomorfológico de una transversal en la Sierra de Gredos Oriental (Sistema Central Español). Ensayo de una cartografia geomorfológica. Ph.D. Thesis, Facultad de Ciencias Geológicas, Universidad Complutense, Madrid.

Garzón Heydt, G.; Tejero, R.; Ortega, J.A. & Garrote, J. (2012). Incisión y desarrollo de la red fluvial sobre sustrato rocoso. Morfología tectónica en el interfluvio Tajo-Guadiana. Actas XII Reunión Nacional de Geomorfología. Santander (Spain).

Gasparini, N.M.; Whipple, K.X. & Bras, R.L. (2007). Predictions of steady state and transient landscape morphology using sedimentflux-dependent river incision models. Journal of Geophysical Research-Earth Surface, 112. https://doi.org/10.1029/2006JF000567

Gladfelter, B.G. (1971). Meseta and campiña landforms in central Spain: a geomorphology of the Alto Henares basin. Department of Geography, University of Chicago.

Goldrick, G. & Bishop, P. (2007). Regional analysis of bedrock stream long profiles: evaluation of Hack's SL form, and formulation of an alternative (the DS form). Earth Surface Processes and Landforms 32: 649-671. https://doi.org/10.1002/esp.1413

Gouveia, M.P.; Cunha, P.P.; Falguères, C.; Voinchet, P.; Martins, A.A.; Bahain, J.-J. & Pereira, A. (2020). Electron spin resonance dating of the culminant allostratigraphic unit of the Mondego and Lower Tejo Cenozoic basins (W Iberia), which predates fluvial incision into the basin-fill sediments. Global and Planetary Change, 184: 103081. https://doi.org/10.1016/j.gloplacha.2019.103081

Gracia, F.J.; Gutiérrez, M. & Leranoz, B. (1988). Las superficies de erosión neógenas en el sector central de la Cordillera Ibérica. Revista Sociedad Geológica de España, 1(1-2): 135-142.

Gutiérrez-Elorza, M. & Gracia, F.J. (1997). Environmental interpretation and evolution of the Tertiary erosion surfaces in the Iberian range (Spain). In: M. Widdowson, (Eds), Palaeosurfaces: Recognition, Reconstruction and Palaeoenvironmental Interpretation. Geological Society Special Publication, 120: 147-158. https://doi.org/10.1144/GSL.SP.1997.120.01.10

Hack, J.T. (1973). Stream-profile analysis and the stream-gradient index. Journal of Research of the United State Geological Survey, 1: 421-429.

Hancock, G.S. & Anderson, R.S. (2002). Numerical modeling of fluvial strath-terrace formation in response to oscillating climate. Geological Society of America Bulletin 114: 1131-1142. https://doi.org/10.1130/0016-7606(2002)114<1131:NMOFST>2.0.CO;2

Hernández-Pacheco, E. (1932). Tres ciclos de erosion geologica en las Sierras Orientales de la Cordillera Central. Boletin Sociedad Española de Historia Natural, 32: 455-460.

Horton, R.E. (1945). Erosional development of streams and their drainage basins: hydrophysical approach to quantitative morphology. The Geological Society of America, 56: 275-370. https://doi.org/10.1130/0016-7606(1945)56[275:EDOSAT]2.0.CO;2

Jena, S.K. & Tiwari, K.N. (2006). Modeling synthetic unit hydrograph parameters with geomorphologic parameters of watersheds. Journal of Hydrology, 319: 1-14. https://doi.org/10.1016/j.jhydrol.2005.03.025

Karampaglidis, T. (2015). La evolución geomorfológica de la cuenca de drenaje del río Lozoya (Comunidad de Madrid, España). Ph.D. Thesis, Universidad Complutense, Madrid.

Karampaglidis, T.; Benito-Calvo, A. & Perez-Gonzalez, A. (2014a). Geomorphology of the Lozoya river drainage basin area (Community of Madrid, Spanish Central System). Journal of Maps, 11(2): 342-353. http://doi.org/10.1080/17445647.2014.926103

Karampaglidis, T.; Benito-Calvo, A. & Perez-Gonzalez, A. (2014b). Analyzing the drainage network combining morphometric indices and statistic tools. A case study from Lozoya River basin (Spanish Central System, Community of Madrid-Guadalajara). 13rd Meeting of the Spanish Society of Geomorphology, Caceres (Spain).

Karampaglidis, T.; Benito-Calvo, A.; Pérez-González, A.; Baquedano, E. & Arsuaga, J.L. (2011). Secuencia geomorfológica y reconstrucción del paisaje durante el Cuaternario en el valle del río Lozoya (Sistema Central, España). Boletín de la Real Sociedad Española de Historia Natural, Sección Geológica, 105(1-4): 149-162.

Karampaglidis, T.; Rodes, A.; Benito-Calvo, A.; Pérez-González, A. & Miguens-Rodriguez, L. (2014c). Exposure ages of two rock terraces of the Lozoya River (Central Spain) from cosmogenic nuclides Be-10 and Al-26. 13rd Meeting of the Spanish Society of Geomorphology, Caceres (Spain).

Karampaglidis, T.; Benito-Calvo, A.; Rodés, A.; Braucher, R.; Pérez-González, A.; Pares, J.; Stuart, F.; Di Nicola, L. & Bourles, D. (2020). Pliocene endorheic-exhoreic drainage transition of the Cenozoic Madrid Basin (Central Spain). Global and Planetary Change, 194: 103295. https://doi.org/10.1016/j.gloplacha.2020.103295.

Knighton, A.D. (1998). Fluvial Forms and Processes. A New Perspective. Arnold, London.

Larue, J.P. (2008). Effects of tectonics and lithology on long profiles of 16 rivers of the southern Central Massif border between the Aude and the Orb (France). Geomorphology, 93: 343-367. https://doi.org/10.1016/j.geomorph.2007.03.003

Leopold, L.B. (1994). A View of the River. Cambridge University Press, New York.

McKnight, T. & Hess, D. (2005). The Fluvial Processes. Physical Geography: A Landscape Appreciation (8th ed.). Pearson, Prentice Hall, New Jersey.

McLachlan, G.,J. (2004). Discriminant analysis and statistical patterns recognition. John Willey & Sons, Hoboken, New Jersey.

Merritts, D.; Vincent, K. & Wohl, E. (1994). Long river profiles, tectonism, and eustasy: A guide to interpreting fluvial terraces. In: Tectonics and Topography (Ellis, M. and Merritts, D., Eds.). Special Section Part II, Journal of Geophysical Research, 99 (B7): 14.031-14.050. https://doi.org/10.1029/94JB00857

Mink, S.; López-Martínez, J.; Maestro, A.; Garrote, J.; Ortega, J.A.; Serrano, E.; Durán, J.J. & Schmid, T. (2014). Insights into deglaciation of the largest ice-free area in the South Shetland Islands (Antarctica) from quantitative analysis of the drainage system, Geomorphology, 225: 4-24. https://doi.org/10.1016/j.geomorph.2014.03.028

Montgomery, D.R. (2004). Observations on the role of lithology in strath terrace formation and bedrock channel width. American Journal of Science 304: 454-476. http://doi.org/10.2475/ajs. 304.5.454.

Morales, J.; Alcalá, L. & Nieto, M. (1993). Las faunas de vertebrados del Terciario. In Madrid antes del hombre. Museo Nacional de Ciencias Naturales. Comunidad de Madrid, 23-31.

Moreno, D.; Falguères, C.; Pérez-González, A.; Duval, M.; Voinchet, P.; Benito-Calvo, A.; Ortega, A.I.; Bahain, J.J.; Sala, R.; Carbonell, E.; Bermúdez de Castro, J.M. & Arsuaga, J.L. (2012). ESR chronology of alluvial deposits in the Arlanzón valley (Atapuerca, Spain): Contemporaneity with Atapuerca Gran Dolina site. Quaternary Geochronology, 10: 418-423. https://doi.org/10.1016/j.quageo.2012.04.018

Morris, P.H. & Williams, D.J. (1997). Exponential longitudinal profiles of streams. Earth Surface Processes and Landforms, 22: 143-163. https://doi.org/10.1002/(SICI)1096-9837(199702)22:2<143::AID-ESP681>3.0.CO;2-Z

Ohmori, H. (1991). Change in the mathematical function type describing the longitudinal profile of a river through an evolutionary process. Journal of Geology 99: 97-110. https://doi.org/10.1086/629476

Ordoñez, S.; González Martín, J.A. & Garcia Del Cura, M.A. (1990). Datacion radiogenica (U-234/U-238 y Th-230/U-234) de sistemas travertinicos del Alto Tajo (Guadalajara). Geogaceta, 8: 53-56.

Ortiz, J.E.; Torres, T.; Delgado, A.; Reyes, E. & Díaz-Bautista, A. (2009). A review of the Tajo river tufa deposits (central Spain): age and palaeoenvironmental record. Quaternary Science Review, 28: 947-963. https://doi.org/10.1016/j.quascirev.2008.12.007

Palacios, D.; De Marcos, J. & Vasquez-Selem, L. (2011). Last Glacial Maximum and deglaciation of Sierra de Gredos, Central Iberian Peninsula. Quaternary International, 233: 16-26. https://doi.org/10.1016/j.quaint.2010.04.029

Pastre, J. (2005). Les nappes alluviales de l'Allier en Limagne (Massif Central, France): stratigraphie et corrélations avec le volcanisme regional. Quaternaire, 16(3): 153-175. https://doi.org/10.4000/quaternaire.383

Patton, P.C. (1988). Drainage basin morphometry and floods. In: Flood Geomorphology (V.R. Baker, R.C. Kochel, and P.C. Patton, Eds.). Wiley, New York, 51-65.

Pazzaglia, F.J.; Gardner, T.W. & Merritts, D. (1998), Bedrock fluvial incision and longitudinal profile development over geologic time scales determined by fluvial terraces, In: Bedrock Channels: American Geophysical Union (Wohl, E. & Tinkler, K., Eds.). Geophysic Monograph Series, 107: 207-235. https://doi.org/10.1029/GM107p0207

Pazzaglia, F.J. (2013). Fluvial terraces. In: Treatise on Geomorphology (Schroeder, J.F., Ed.). Elsevier, 379-412. https://doi.org/10.1016/B978-0-12-374739-6.00248-7

Pedraza, J. (1994). El sistema Central Español. In: Geomorfología de España (M. Gutiérrez Elorza, Eds.). Rueda, Madrid, 63-100.

Pedraza, J. & Carrasco, R.M. (2005). El Glaciarismo Pleistoceno del Sistema Central. Enseñanza de las Ciencias de la Tierra, 13(3): 278-288.

Pedraza, J. (1978). Estudio geomorfológico de la zona de enlace entre las Sierras de Gredos y Guadarrama (Sistema Central Español). Ph.D. Thesis, Universidad Complutense, Madrid.

Pedrera, A.; Vicente Pérez-Peña, J.; Galindo-Zaldívar, J.; Miguel Azañón, J. & Azor, A. (2009). Testing the sensitivity of geomorphic indices in areas of low-rate active folding (eastern Betic Cordillera, Spain). Geomorphology, 105: 218-231. https://doi.org/10.1016/j.geomorph.2008.09.026

Pérez-González, A. (1994). Depresión del Tajo. In: Geomorfologia de España (Gutierrez Elorza, M., Ed.). Rueda, Madrid, 389-410.

Pérez-González, A.; Gallardo-Millán, J.L.; Uribelarrea, D.; Panera, J. & Rubio-Jara, S. (2013). La inversion Matuyama-Brunhes en la secuencia de terrazas del río Jarama entre Velilla de San Antonio y Altos de la Mejorada, al SE de Madrid (España). Estudios Geológicos, 69(1):35-46. https://doi.org/10.3989/egeol.40862.173

Pérez-González, A.; Karampaglidis, T.; Arsuaga, J.L.; Baquedano, E.; Bárez, S.; Gómez, J.J.; Panera, J.; Márquez, B.; Laplana, C.; Mosquera, M.; Huguet, R.; Sala, P.; Arriaza, M.C.; Benito, A.; Aracil, E. & Maldonado, E. (2010). Aproximación geomorfológica a los yacimientos del Pleistoceno Superior del Calvero de la Higuera en el Valle Alto del Lozoya (Sistema Central español, Madrid). In: Actas de la primera

reunión de científicos sobre cubiles de hienas (y otros grandes carnívoros) en los yacimientos arqueológicos de la Península Ibérica. Zona Arqueológica 13 (E. Baquedano & J. Rossell, Eds.). Alcalá de Henares, Museo Arqueológico Regional, Madrid.

Pérez-Peña, J.S.; Azor, A.; Azañón, J.M. & González-Lodeiro, F. (2009). Spatial analysis of stream power using GIS: SLk anomaly maps. Earth Surface Processes and Landforms 34: 16- 25. https://doi.org/10.1002/esp.1684

Personius, S.F.; Kelsey, H.M. & Grabau, P.C. (1993). Evidence for regional stream aggradation in the Central Oregon Coast range during the Pleistocene-Holocene transition. Quaternary Research, 40: 297-308. http://doi.org/10.1006/qres.1993.1083

Phillips, J.D. & Lutz, J.D. (2008). Profile convexities in bedrock and alluvial streams. Geomorphology, 102 (3-4): 554-566. https://doi.org/10.1016/j.geomorph.2008.05.042

Pinilla, L.; Pérez-González, A.; Sopeña, A. & Pares, J.M. (1995). Fenómenos de hundimientos sinsedimentarios en los depósitos cuaternarios del río Tajo en la cuenca de Madrid (Almoguera-Fuentidueña de Tajo). In: Reconstrucción de paleoambientes y cambios climáticos durante el Cuaternario (Aleixandre, T. & Pérez-González, A., Eds.). Centro de Ciencias Medioambientales. CSIC, Madrid, 125-139.

Portero, J.M.; Díaz, M.; González, F.; Pérez, A.; Gallardo, J.; Aguilar, M.J. & Leal, M.C. (1990). Mapa Geológico de España 1:50,000, sheet 485 (Valdepeñas de la Sierra). IGME. Madrid.

Prince, P.S.; Spotila, J.A. & Henika, W.S. (2011). Stream capture as driver of transient landscape evolution in a tectonically quiescent setting. Geology 39(9): 823-826. https://doi.org/10.1130/G32008.1

Richards, K.S. (1982). Rivers. Form and Process in Alluvial Channels. Edward Arnold, London.

Ritter, D.F.; Kochel, R.C. & Miller, J.R. (1995). Process Geomorphology. William C. Brown, Dubuque, Iowa.

Roe, G.H.; Montgomery, D.R. & Hallet, B. (2002). Effects of orographic precipitation variations on the concavity of steady state river profiles. Geology 30: 143-146. https://doi.org/10.1130/0091-7613(2002)030<0143:EOOPVO>2.0.CO;2

Rodríguez-Rodríguez, L.; Antón, L.; Rodés, Á.; Pallàs, R.; García-Castellanos, D.; Jiménez Munt, I.; Struth, L.; Leanni, L. & ASTER Team (2020). Dates and rates of endo-exorheic drainage development: Insights from fluvial terraces (Duero River, Iberian Peninsula). Global and Planetary Change, 193: 103271. http://doi.org/10.1016/j.gloplacha.2020.103271

Santisteban, J.I. & Schulte, L. (2007). Fluvial networks of the Iberian Peninsula: a chronological framework. Quaternary Science Reviews, 26: 2738-2757. https://doi.org/10.1016/j.quascirev.2006.12.019

Santonja, M. & Pérez-González, A. (1997). Los yacimientos achelenses en terrazas fluviales de la Meseta Central española. In: Cuaternario Ibérico (Rodríguez. J Vidal, Ed.). Comunidad de Madrid, Madrid, 224-234.

Santonja, M. & Pérez-González, A. (2001). El Paleolítico inferior en el interior de la Península Ibérica. Un punto de vista desde la Geoarqueologia. Zephyrus: 53-54(2000-2001): 27-77.

Schanz, S.A. & Montgomery, D.R. (2016). Lithologic controls on valley width and strath terrace formation. Geomorphology, 258: 58-68. https://doi.org/10.1016/j.geomorph.2016.01.015

Schumm, S.A. (2005). River Variability and Complexity. Cambridge University Press, New York. https://doi.org/10.1017/CBO9781139165440

Schwenzner, J. (1937). La región montañosa central de la meseta española. Resumen de la obra: Zur Morphologie des Zentral-spanischen Hochlandes. Geographische Abhandlungen. Boletín de la Sociedad Española de Historia Natural, 41: 121-147.

Seong, Y.B.; Owen, L.A.; Bishop, M.P.; Bush, A.; Clendon, P.C.; Luke, F.; Robert, C.; Kamp, U. & Shroder, J.F. (2008). Rates of fluvial bedrock incision within an actively uplifting orogen: Central Karakoram Mountains, northern Pakistan. Geomorphology, 97 (3-4): 274-286. https://doi.org/10.1016/j.geomorph.2007.08.011

Sesé, C. & Ruiz, A. (1992). Nuevas faunas de micromamíferos del Pleistoceno del Norte de la Provincia de Madrid (España). Boletín de la Real Sociedad Española de Historia Natural (Sección Geología), 87 (1-4): 115-139.

Silva, P.G.; Goy, J.L. & Zazo, C. (1988). Neotectónica del sector centro-meridional de la Cuenca de Madrid. Estudios Geológicos, 44: 415-427. https://doi.org/10.3989/egeol.88445-6558

Silva, P.G. & Ortiz, I. (2002). Mapa geomorfológico. In: Mapa Geológico de España, E1:50,000, (Ledanca (487). IGME, Madrid.

Silva, P.G.; Roquero, E.; López-Recio, M.; Huerta, P. & Martínez-Graña, A.M. (2017). Chronology of fluvial terrace sequences for large Atlantic rivers in the Iberian Peninsula (Upper Tajo and Duero drainage basins, Central Spain). Quaternary Science Reviews, 166: 188-203. https://doi.org/10.1016/j.quascirev.2016.05.027

Sinha, S.K. & Parker, G. (1996). Causes of concavity in longitudinal profiles of rivers. Water Resources Research, 32: 1417-1428. https://doi.org/10.1029/95WR03819

Smith, T.R.; Merchant, G.E. & Birnir, B. (2000). Transient attractors: towards a theory of the graded stream for alluvial and bedrock channels. Computers and Geosciences, 26: 541-580. https://doi.org/10.1016/S0098-3004(99)00128-4

Snow, R.S. & Slingerland, R.L. (1987). Mathematical modeling of graded river profiles. Journal of Geology 95, 15-33. https://doi.org/10.1086/629104

Snyder, N.P.; Whipple, K.X.; Tucker, G.E. & Merritts, D.J. (2000). Landscape response to tectonic forcing: digital elevation model analysis of stream profiles in the Mendocino triple junction region, northern California. Geological Society of America Bulletin 112: 1250-1263. https://doi.org/10.1130/0016-7606(2000)112<1250:LRTTFD>2.0.CO;2

Soria-Jáuregui, A.; Jiménez-Cantizano, F. & Antón, L. (2018). Geomorphic and tectonic implications of the endorheic to exorheic transition of the Ebro River system in Northeast Iberia. Quaternary Research, 91(2) : 472-492. https://doi.org/10.1017/qua.2018.87.

Stock, J.D.; Montgomery, D.R.; Collins, B.D.; Dietrich, W.E. & Sklar, L. (2005). Field measurements of incision rates following bedrock exposure: implications for process controls on the long profiles of valleys cut by rivers and debris flows. Geological Society of America Bulletin 117: 174-194. http://doi.org/10.1130/B25560.1

Stokes, M.; Mather, A.E.; Belfoul, M.; Faik, F.; Bouzid, S.; Geach, M.R.; Cunha, P.P.; Boulton, S.J. & Thiel, C. (2017). Controls on dryland mountain landscape development along the NW Saharan desert margin: Insights from Quaternary river terrace sequences (Dadès River, south-central High Atlas, Morocco). Quaternary Science Reviews, 166: 363-379. https://doi.org/10.1016/j.quascirev.2017.04.017

Strahler, A.N. (1964). Quantitative geomorphology of drainage basins and channel networks. In: Handbook of Applied Hydrology (V.T. Chow, Eds.). McGraw-Hill, New York.

Struth, L.; Garcia-Castellanos, D.; Viaplana-Muzas, M. & Vergés, J. (2019). Drainage network dynamics and knickpoint evolution in the Ebro and Duero basins: from endorheism to exorheism. Geomorphology 327: 554-571. https://doi.org/10.1016/j.geomorph.2018.11.033.

Torres, T.; Cobo, R.; García-Alonso, P.; Grün, R.; Hoyos, M.; Juliá, R.; Llamas, J. & Soler, V. (1995). Evolución del sistema fluvial Jarama-Lozoya-Guadalix durante el Plioceno terminal y Cuaternario. Geogaceta, 17: 46-48.

Torres, T.; Ortiz, J.E.; Cobo, R.; Puch, C.; Julia, R.; Grün, R. & Soler, V. (2005). Génesis y edad del karst del Cerro de la Oliva y la Cueva del Reguerillo (Torrelaguna, Madrid). Libro homenaje al Profesor D. Rafael Fernández Rubio, Madrid.

Türkan, A. & Bekir, A. (2011). Development and morphometry of drainage network in volcanic terrain, Central Anatolia, Turkey. Geomorphology, 125(4): 485-503. https://doi.org/10.1016/j.geomorph.2010.09.023

Turowski, J.M.; Hovius, N.; Meng-Long, H.; Lague, D. & Men-Chiang, C. (2008). Distribution of erosion across bedrock channels. Earth Surface Processes and Landforms, 33: 353-363. http://dx. doi.org/10.1002/esp.1559

Turowski, J.M.; Lague, D. & Hovius, N. (2007). Cover effect in bedrock abrasion: a new derivation and its implications for the modeling of bedrock channel morphology. Journal of Geophysical Research Earth Surface, 112: F04006. http://doi.org/10.1029/2006JF000697

Van den Berg, M.W. & van Hoof, T. (2001). The Maas terrace sequence at Maastricht, SE Netherlands: evidence for 200 m of late Neogene and Quaternary surface uplift. In: River Basin Sediment Systems (Maddy, D.; Macklin, M.G. & Woodward, J.C., Eds.), Archives of Environmental Change. Balkema, Abingdon, England, 45-86.

Vicente, G. De; Cloetingh, S.; Van Wees, J.D. & Cunha, P. (2011). Tectonic classification of Cenozoic Iberian foreland basins. Tectonophysics, 502, 38-61. https://doi.org/10.1016/j.tecto.2011.02.007

Vicente, G. De; Vegas, R.; Muñoz-Martín, A.; Silva, P.G.; Andrienssen, P.; Cloetín, S.; González-Casado, J.M.; Van Wees, J.D.; Alvárez, J.; Carbó, A. & Olaiz, A. (2007). Cenozoic thick-skinned deformation and topography evolution of the Spanish Central System. Global and Planetary Change, 58: 335-381. https://doi.org/10.1016/j.gloplacha.2006.11.042

Vijith, H. & Satheesh, R. (2006). GIS based morphometric analysis of two major upland sub-watersheds of Meenachil River in Kerala (short note). Journal of the Indian of Remote Sensing, 34: 181-185. https://doi.org/10.1007/BF02991823

Vijith, H.; Prasannakumar, V.; Sharath Mohan, M.A.; Ninu Krishnan M.V. & Pratheesh, P. (2017) River and basin morphometric indexes to detect tectonic activity: a case study of selected river basins in the South Indian Granulite Terrain (SIGT). Physical Geography, 38 (4): 360-378. https://doi.org/10.1080/02723646.2017.1283478

Warburton, J. & Álvarez, C. (1989). A thrust tectonic interpretation of the Guadarrama Mountains, Spanish Central System. In: Libro Homenaje a Chow (Libro Homenaje a R. Soler, Eds.). Asociación de Geólogos y Geofísicos Españoles del Petróleo (AGGEP), Madrid.

Wegmann, K.W. & Pazzaglia, F.J. (2002). Holocene strath terraces, climate change, and active tectonics: the Clearwater River basin, Olympic Peninsula, Washington State. Geological Society of America Bulletin 114: 731-744. http://doi.org/10.1130/0016-7606(2002)114b0731: HSTCCAN2.0.CO;2

Wells, S.G.; Bullard, T.F.; Menges, T.M.; Drake, P.G.; Karas, P.A.; Kelson, K.I.; Ritter, J.B. & Wesling, J.R. (1988). Regional variations in tectonic geomorphology along segmented convergent plate boundary, Pacific coast of Costa Rica. Geomorphology, 1: 239-265. https://doi.org/10.1016/0169-555X(88)90016-5

Westaway, R. (2006). Investigation of coupling between surface processes and induced flow in the lower continental crust as a cause of intraplate seismicity. Earth Surface Processes and Landforms, 31: 1480-1509. https://doi.org/10.1002/esp.1366

Westaway, R.; Bridgland, D.R.; Sinham, R. & Demir, T. (2009). Fluvial sequences as evidence for landscape and climatic evolution in the Late Cenozoic: A synthesis of data from IGCP 518. Global and Planetary Change, 68 (4): 237-253. https://doi.org/10.1016/j.gloplacha.2009.02.009

Westaway, R.; Maddy, D. & Bridgland, D. (2002). Flow in the lower continental crust as a mechanism for the Quaternary uplift of south-east England: constraints from the Thames terrace record. Quaternary Science Reviews, 21: 559-603. https://doi.org/10.1016/S0277-3791(01)00040-3

Whipple, K.X. (2004). Bedrock rivers and the geomorphology of active orogens. Annual Review of Earth & Planetary Sciences, 32: 151-185. https://doi.org/10.1146/annurev.earth.32.101802.120356

Yanites, B.J. & Tucker, G.E. (2010). Controls and limits on bedrock channel geometry. Journal of Geophysical Research Earth Surface, 115: F04019. http://doi.org/10.1029/2009JF001601